

Edge of entanglement in non-ergodic states: a complexity parameter formulation

Devanshu Shekhar and Pragya Shukla

*Department of Physics, Indian Institute of Technology,
Kharagpur-721302, West Bengal, India*

(Dated: December 11, 2024)

arXiv:2310.12796v2 [quant-ph] 10 Dec 2024

Abstract

We analyse the subsystem size scaling of the entanglement entropy of a non-ergodic pure state that can be described by a multi-parametric Gaussian ensemble of complex matrices in a bipartite basis. Our analysis indicates, for a given set of global constraints, the existence of infinite number of universality classes of local complexity, characterized by the complexity parameter, for which the entanglement entropy reveals a universal scaling with subsystem size. A rescaling of the complexity parameter helps us to identify the critical regime for the entanglement entropy of a broad range of pure non-ergodic states.

I. INTRODUCTION

Random quantum states, engineered or that of a physical observable, belong to an important class that are increasingly making their robust appearance in many domains [1–5]. For example, with quantum entanglement used as a resource, the engineering of quantum states to achieve specific objectives for quantum information processing has become an active area of research [1, 2]. Contrary to quantum states of a physical observable, e.g., Hamiltonian, the states used in quantum information can consist of components determined by their proposed function/utility (subject to normalization condition), and evolve under unitary gate operations. Indeed a typical processing unit in quantum information and communication studies can consist of single or multiple layers of quantum gates/ channels (e.g., a quantum circuit) and often use the initial state as the engineered random state of many interacting qubits. As indicated by many studies in past, it is often advantageous to consider random gates (e.g., for quantum error correction [6, 7]). This however leads to a randomization of the incoming state $|\Psi_{in}\rangle$, with nature and type of the randomness dependent on the choice of the unitary operator U as well as $|\Psi_{in}\rangle$: $|\Psi_{out}\rangle = U|\Psi_{in}\rangle$. Due to presence of many gates usually, a typical component of the outgoing state consists of a sum over many random variables and by invoking central limit theorem, its distribution can often be predicted as a Gaussian. But the distribution parameters of the components can in general differ; this in turn leads to a representation of the state by a multiparametric Gaussian density. Even in case of non-random gates, a state used for realistic communication purposes has to transmit through noisy channels; this in turn randomizes the components. For cases, where the effect of noise leaves the information only about the first two moments, the maximum entropy

hypothesis (MEP) permits the components to be described by independent (need not be identical though) Gaussian distributions subject to normalization condition. This motivates the present work, with a primary focus to numerically analyse the bipartite entanglement aspects of a specific class of such states, namely, pure states with Gaussian components.

The manifestation of randomness in a natural quantum state (e.g of a physical observable) can intuitively be explained as follows. A quantum state often reflects the complexity of the system, with its dynamics expected, in general, to be sensitive to many system parameters, quantifying the local constraints, e.g., disorder and global constraints, e.g., symmetry, conservation laws etc. Although inherently probabilistic in nature, its components in a Hilbert space basis can be determined to a reasonable accuracy, e.g., if the eigenstates and eigenvalues of an operator, e.g., Hamiltonian can be determined exactly. A lack of detailed information due to complexity renders an exact determination of the components in a physically motivated basis technically difficult, often leaving them best described by a distribution even in absence of disorder. The nature and type of the randomness can again be determined by invoking maximum entropy hypothesis under known system constraints, e.g., symmetry, conservation laws, disorder, dimensionality etc.

While a consideration of independent Gaussian distributed components for realistic quantum states may seem to have limited applications, however, as revealed by previous studies of the Hermitian ensembles representing a wide range of complex systems, this seems to be a good approximation. For example, almost all components of a typical state of a quantum chaotic system can be described by independent, identical Gaussian distributions subjected to normalization condition (as corroborated by the success of well-known Porter Thomas distribution of local intensity for quantum chaotic states) [8] (also discussed in [9]). We recall that, notwithstanding the normalization condition subjecting the sum of the components to a fixed value, the components can still be statistically uncorrelated and therefore described by independent distributions. A Gaussian behaviour of the eigenfunctions components is also indicated by the study [10] for Rosenzweig-Porter ensemble (matrix elements Gaussian distributed with zero mean and a fixed ratio of diagonal to off-diagonal variances); the latter is believed to be a good model for many body localization \rightarrow delocalization transition, if subjected to an additional constraint of fixed diagonals. In absence of the latter, the components remain independent although their behaviour in the bulk is only approximately Gaussian (see eq.(20) of [10]). Indeed the observed Gaussian behaviour of the components

numerically motivated consideration of the Hilbert-Schmidt ensembles for generic quantum states and in the investigation of any quantum information processing task, it is always desirable to make use of generic Gaussian states to benchmark the performance [11]. For example, some of the well known quantum states of light, playing important role in optical communication are fermionic Gaussian states which also consist of Gaussian components [12, 13].

Based on prevailing system conditions, a quantum system can in general be in an ergodic or non-ergodic state. While an ergodic state is typically attributed to strong quantum correlations, e.g., high degree of entanglement [14], the latter can vary among different non-ergodic states of a given system. The changing system conditions, e.g., variation of disorder strength and/or many-body interactions, can also affect the correlations leading to a crossover from localized \rightarrow non-ergodic extended \rightarrow delocalized state, or separable \rightarrow entangled \rightarrow maximally entangled states in the bipartite basis. More specifically, the entanglement entropy can evolve with changing system conditions, from zero (separable) to a maximum possible limit, with the rate of evolution in general dependent on many system parameters. As mathematical derivations are often based on system-specific approximations, this renders a theoretical formulation of the entanglement entropy of non-ergodic states, applicable under all possible system conditions, a technically challenging task. It is therefore desirable if possible to identify the classes of non-ergodic states for which a common mathematical formulation of the entanglement measures can be derived. An important theoretical insight in this context was given in [15], implying that a controlled variation of the entanglement of a specific class of non-ergodic random states (those with multiparametric Gaussian distributed components), between zero and a maximum limit, can be achieved by varying just a single functional of the system parameters, hereafter referred as the complexity parameter. The primary objective of the present work is to pursue the insight further, numerically analyse its implication and establish that a size based rescaling of the complexity parameter not only helps in identifying the universality classes of the ensemble averaged entanglement entropy but also reveals its critical regime. We note that the scaling of entanglement entropies [16] of a quantum state with sub-system size is a topic of immense interest in various many-body physics contexts, e.g., seeking criticality in local quantum systems [17], understanding the topological properties of ground states [18], pinpointing quantum phase transition point in systems driven by a quenched disorder parameter [19–22], and for establishing connection

between quantum mechanics and gravity [23]. While the scaling behaviour in case of ergodic states is believed to be well-understood [14] (with the entanglement entropy scales as the volume of the subsystem), many aspects of the non-ergodic pure states are still not properly understood. The criticality of entanglement too has many ramifications, e.g., in the study of phase transitions of many-body systems.

The paper is organized as follows. As our search for the above mentioned universality is based on the complexity parameter formulation [15], it is briefly reviewed in section II to keep the paper self-contained. The section also specifies the specific class of non-ergodic quantum states, to which our theoretical formulation is applicable. An important aspect of the formulation i.e the role of constants of evolution, not well-emphasized in [15], is also now elaborated. A few misprints appeared in [15] are also now corrected. Section III B and III C describe the numerical analysis of the universality and criticality of the average entanglement entropy for a few state matrix ensembles with different variance structures but for two subsystems of equal sizes. To understand the influence of subsystem size on universality, section III D analyses the case with different subsystems sizes. We conclude in section IV with main results and open questions.

II. COMPLEXITY PARAMETER FORMULATION OF THE EVOLUTION: A BRIEF REVIEW

Consider a pure bipartite quantum state $|\Psi\rangle = \sum C_{kl} |a_k\rangle |b_l\rangle$ with coefficients C_{kl} (complex or real) as a measure of the correlations between the orthogonal subspaces of its sub parts A and B , consisting of basis vectors $|a_k\rangle$ and $|b_l\rangle$, $k = 1 \rightarrow N_A, l = 1 \rightarrow N_B$ respectively. The standard entanglement measures for a pure bipartite state, viz., the von Neumann R_1 and other Rényi entropies R_n with $n > 1$, are functions of the eigenvalues of the $N_A \times N_A$ reduced density matrix for A as $W = C \cdot C^\dagger$ (also known as Schmidt eigenvalues). For notational ease, hereafter we use $N_A = N$ and $N_B = N + \nu_0$.

A real physical system is in general subject to many global constraints, e.g., symmetries and conservation laws. In presence of exact discrete symmetries and if the quantum state preserves them, the physically motivated basis to study the dynamics is the one that preserves the symmetry. The eigenstate in a symmetry resolved basis, can be written as products of the eigenfunctions of different symmetry blocks. The state matrix C in such

a basis will however appear in a block diagonal form, with each block symmetry resolved, i.e., related to a symmetry related quantum number. As the latter are independent, it is appropriate to confine the entanglement analysis to one of the symmetry resolved blocks. The Schmidt eigenvalues for one such block can only have accidental degeneracy, also known as avoided crossings. (This is discussed in detail in [9, 24] in context of Hermitian matrices in general). Besides a consideration of the state matrix with no symmetries is relevant in context of an engineered quantum state too. For clarity of presentation of our ideas, here we assume that the state $|\Psi\rangle$ is not subjected to any discrete symmetry constraints.

A. Ensemble Density

As mentioned in section I, a lack of exact determination of the components due to underlying complexity leaves their statistical description as the best option. A quantum state with random components is best described by an ensemble of exact replicas of the state matrix. The nature and type of the ensemble representing a random quantum state depends on the nature of its dynamics in the chosen basis. While an ergodic state can be well-represented by a basis-independent ensemble, the non-ergodicity requires the ensemble to be basis dependent. Here we consider an ensemble of state matrices representing a wide range of non-ergodic states. Referring the joint probability density function (JPDF) of the components C_{kl} as $\rho_{cn}(C; h, b)$ (also known as the ensemble density), it can be expressed as

$$\rho_{cn}(C; h, b) = \rho_c(C; h, b) \delta\left(\sum |C_{kl}|^2 - 1\right) \quad (1)$$

where $\rho_c(C; h, b)$ describes the JPDF of the state without normalization constraint.

To determine the average behaviour of R_n from eq.(1), we proceed as follows. The JPDF $\rho_w(W)$ of the reduced density matrix W can be expressed as

$$\rho_w(W) = \int \delta(W - C \cdot C^\dagger) \rho_{cn}(C; h, b) DC \quad (2)$$

$$= \delta(\text{Tr } W - 1) \int \delta(W - C \cdot C^\dagger) \rho_c(C; h, b) DC \quad (3)$$

As a consequence of randomized W , the Schmidt eigenvalues and thereby entanglement measures can fluctuate over the ensemble (from one sample to another) and it is necessary to consider their distribution over the ensemble. Defining the eigenvalues of W as e_1, \dots, e_N ,

the JPDF $P_c(\lambda_1, \dots, \lambda_N)$ of the n^{th} eigenvalue to lie between $\lambda_n \rightarrow \lambda_n + d\lambda_n$ (for $n = 1 \rightarrow N$) can be given as

$$P_c(\lambda_1, \dots, \lambda_N) = \int \prod_{n=1}^N \delta(\lambda_n - e_n) \rho_w(W) DW \quad (4)$$

$$= C_{hs} \delta\left(\sum_n \lambda_n - 1\right) P_\lambda(\lambda_1, \dots, \lambda_N) \quad (5)$$

with $P_\lambda(\lambda_1, \dots, \lambda_N) = \int \prod_{n=1}^N \delta(\lambda_n - e_n) \delta(W - C \cdot C^\dagger) \rho_c(C; h, b) DC DW$. Here C_{hs} is a normalization constant: choosing $\int \delta(\sum_n \lambda_n - 1) P_\lambda(\lambda_1, \dots, \lambda_N) D\lambda = 1/C_{hs}$ renders P_c normalized to unity: $\int P_c D\lambda = 1$ with $D\lambda \equiv \prod_{n=1}^N d\lambda_n$.

While, similar to a non-random state, the entanglement entropy of a single sample of a random state too does not depend on the basis, but its ensemble average can in general depend on the ensemble parameters. This can be seen from following expression for average entanglement entropy [15],

$$\langle R_n \rangle = \int R_n(\lambda_n) \delta\left(S_1 - \sum_n \lambda_n\right) P_\lambda D\lambda \quad (6)$$

with $R_1(\lambda_n) = -\sum_n \lambda_n \log \lambda_n$, $R_2 = -\log(\sum_n \lambda_n^2)$ and S_1 is an arbitrary constant constraint on the trace, later to be set as $S_1 = 1$.

As the components C_{kl} are measures of the complicated correlations between the two sub-parts, their determination for generic system conditions can often be technically non-trivial and may involve statistical errors. Besides even if the components of the initial state say $|\Psi(0)\rangle$ are known exactly, a transmission through a quantum channel in presence of an uncontrollable environment may randomize the state: $|\Psi(t)\rangle = U(t, 0)|\Psi(0)\rangle$ with U as the random unitary operator describing the time-evolution of the state. This gives $C_{kl}(t) = \sum_{ij} U_{kl;ij} C_{ij}(0)$ where $U_{kl;ij} \equiv \langle a_k b_l | U | a_i b_j \rangle$ are random variables (subject to unitary constraint). Thus, for non-random components at time $t = 0$, their coupling with U randomizes them for later times; invoking central limit theorem then predicts them to be Gaussian distributed if e.g., $U_{kl;ij}$ are random variables with finite second moments. This motivates us to consider, in present study, the case in which C_{kl} are best known up to their mean and variances only and subjected to normalization condition $\sum_{k,l} |C_{kl}|^2 = 1$. Based on maximum entropy hypothesis, the joint probability density function (JPDF) of

the components can then be given by eq.(1) with

$$\rho_c(C; h, b) \propto \exp \left[- \sum_{k,l,s} \frac{1}{2h_{kl;s}} (C_{kl;s} - b_{kl;s})^2 \right] \quad (7)$$

with $C_{kl} = C_{kl,1} + i C_{kl,2}$ with $k = 1 \rightarrow N, l = 1 \rightarrow N + \nu_0$ and $s = 1, 2$. An important point worth emphasizing here is as follows: while C_{kl} are not independent due to normalization condition, their distributions can still be uncorrelated; this is indeed the idea used in the theory of random ergodic states (see [8]) or Berry's random wave conjecture of [25, 26].

Eq.(1) along with eq.(7) describes a multiparametric Gaussian ensemble of state matrices representing a normalized pure state in a bipartite basis. As the ensemble parameters are a measure of the fluctuations of the components (e.g., due to estimation error or in presence of disorder) different choices of parametric matrices $h \equiv [h_{kl;s}]$ and $b \equiv [b_{kl;s}]$ can correspond to different pure states. For example, using limit of a Gaussian as a δ -function, we have $\lim_{h \rightarrow 0} \rho_c(C) \rightarrow \delta(C - b)$ (with $\lim_{h \rightarrow 0}$ implying $h_{kl;s} \rightarrow 0 \forall k, l, s$); the limit therefore leads to a non-random state. Similarly a choice of $h_{kl;s} \rightarrow \alpha_k \delta_{l1}$ and $b_{kl;s} \rightarrow 0 \forall k, l, s$ gives a typical state of the ensemble separable in the chosen bipartite basis: $|\Psi\rangle = |\Phi_A\rangle |B_1\rangle$ where $|\Phi_A\rangle \sim \sum_{k=1}^{N_A} \alpha_k |\alpha_k\rangle$ is a state in A -subspace. (We note that a separable state in general corresponds to each component written as a product i.e., $C_{kl} = \alpha_k \beta_l$. Assuming both α_k as well as β_l as non random, the pdf of C_{kl} can be expressed as $\delta(C_{kl} - \alpha_k \beta_l) = \lim_{v \rightarrow 0} e^{-\frac{(C_{kl} - \alpha_k \beta_l)^2}{2v}}$. Alternatively, a Gaussian distribution for C_{kl} , for the case in which α_k and β_l are randomly distributed real variables with their PDFs as ρ and σ , can arise if following condition is satisfied: $\sigma(\beta_l) = \int \exp \left[-\frac{\alpha_k^2 \beta_k^2}{2h_{kl}} \right] \rho(\alpha_k) d\alpha_k$; here C_{kl} is assumed real with its mean zero to simplify explanation without any loss of generality).

In general, a non-ergodic random state can consist of components non-Gaussian, non-identically distributed (e.g., both Gaussian and non-Gaussian as well as a few of them non-random too) or even correlated. A theoretical analysis of a generic non-ergodic random states including all cases is however not only technically complicated but also time consuming. While eq.(1) represents only a class of non-ergodic random states, it still represents their wide range and its analysis can help us to gain insights for more generic cases. This motivates us to keep the present analysis confined to only cases represented by the ensemble density of the above type.

B. Complexity Parameter Formulation

The contact with the environment subjects a physical system to many perturbations, often causing a variation of system parameters with time. The latter in general affects the state of the system and, thereby matrix elements C_{kl} , resulting in an evolution of ρ_c in matrix space. But, for ρ_c to represent one of the quantum states, it is necessary that the ensemble parameters take into account all system-specifics, thereby rendering them to be functions of the system parameters. Consequently, they also vary, leading to an evolution of ρ_c in the $\{h_{kl}, b_{kl}\}$ space too. For the evolving ensemble to continue representing the system, it is desirable that the evolution of ρ_c in matrix space is exactly mimicked by that in ensemble parameter space. As discussed in detail in [15, 27] (also see *appendix E*), indeed a constant diffusion of ρ_c in the matrix space, with a drift under harmonic potential, can be exactly described by a specific combination of the first order variation of the ensemble parameters.

The multiparametric evolution can further be simplified by a transformation from M dimensional space $b_{kl;s}, h_{kl;s}$ to another space Y_1, \dots, Y_M that maps the JPDF in eq.(7) to $\rho(H; Y_1, Y_2, \dots, Y_M)$ and leads to its single parametric evolution [15],

$$\frac{\partial \rho}{\partial Y_1} = L\rho, \quad \frac{\partial \rho}{\partial Y_\alpha} = 0 \quad (\alpha > 1) \quad (8)$$

with $L = \sum_{k,l,s} \frac{\partial}{\partial C_{kl;s}} \left[\frac{\partial}{\partial C_{kl;s}} + \gamma C_{kl;s} \right]$ and $\rho = \mathcal{N}_0 \rho_c$ with \mathcal{N}_0 as a constant [15]. Here γ is an arbitrary non-zero parameter, related to variance of C_{kl} in equilibrium limit. We note $\gamma = 0$ corresponds to an evolution with no equilibrium limit.

As discussed in *appendix E*, Y_1 can be obtained by solving a set of characteristic equations, $\frac{dh_{kk;s}}{f_{kk;s}} = \dots = \frac{dh_{kl;s}}{f_{kl;s}} = \frac{db_{kl;s}}{b_{kl;s}} = \frac{dY_\alpha}{\delta_{\alpha 1}}$ with $f_{kl;s} \equiv |2(1 - \gamma h_{kl;s})|$; the solution can be given as

$$Y_1 = -\frac{1}{2M\gamma} \sum'_{k,l,s} (\ln f_{kl;s} + \gamma \ln |b_{kl;s}|^2) + \text{const.}, \quad (9)$$

where the notation $\sum'_{k,l}$ implies a sum over $h_{kl;s} \neq \gamma^{-1}$ and $b_{kl;s} \neq 0$ only [15]. We note that for the evolution occurring in the neighbourhood of $b_{kl} = 0$, or $h_{kl;s} \rightarrow \gamma^{-1}$ the corresponding parametric derivative does not contribute to Y_1 (discussed in more detail in *appendix E*).

With $\frac{\partial \rho}{\partial Y_\alpha} = 0$ for $n > 1$, Eq.(8) implies an evolution of the JPDF $\rho(C)$ in terms of Y_1 subjected to $M - 1$ constants of evolution, namely, Y_2, \dots, Y_M . As discussed in *appendix E*, Y_α , for $\alpha > 1$ can be obtained by solving the eq.(E3).

As discussed in detail in [15], eq.(8) along with eq.(3) and eq.(5) can further be used to derive the Y -governed evolution of the reduced density matrix $\rho_A \equiv C \cdot C^\dagger$ and thereby Schmidt eigenvalues,

$$\frac{\partial P_\lambda}{\partial Y_1} = \mathcal{L}_\lambda P_\lambda, \quad \frac{\partial P_\lambda}{\partial Y_\alpha} = 0, \quad (\alpha > 1) \quad (10)$$

where $\mathcal{L}_\lambda \equiv \sum_{n=1}^N \left[\frac{\partial^2 (\lambda_n P_\lambda)}{\partial \lambda_n^2} - \frac{\partial}{\partial \lambda_n} \left(\sum_{m=1}^N \frac{\beta \lambda_n}{\lambda_n - \lambda_m} + \frac{\beta(\nu_0+1)}{2} - 2\gamma \lambda_n \right) P_\lambda \right]$ and $\nu_0 = N_B - N_A$. Here $\beta = 2$ for C as a complex matrix; (as discussed in [15], $\beta = 1$ for C as a real matrix but the numerical analysis in present study is confined to $\beta = 2$ case only). We note that Y_1 was replaced by Y in [15] for clarity purposes. As discussed in *appendix D*, the level repulsion term (also known as avoided crossing) in the above equation plays an important role in the evolution of Schmidt eigenvalues. Indeed, in separability limit, all eigenvalues except one of them are zero; in maximally entangled limit of the ensemble, eigenvalues are separated by a mean level spacing. The evolution of a typical eigenvalue between the two limits is significantly influenced by the level repulsion term.

Eq.(6) along with the above equation leads to the complexity parameter governed evolution equation for $\langle R_n \rangle(\Lambda, Y_2, \dots, Y_M, S_1)$ (discussed in [15] and referred hereafter as $\langle R_n \rangle(\Lambda, S_1)$ for brevity). Although technically complicated for finite N case, the equation can be simplified in limit $N \rightarrow \infty$, leading to

$$\frac{2}{\beta} \frac{\partial \langle R_n \rangle}{\partial \Lambda} = g_n(\Lambda, S_1) - \frac{\partial \langle R_n \rangle}{\partial S_1}, \quad \frac{\partial \langle R_n \rangle}{\partial Y_\alpha} = 0, \quad (\alpha > 1) \quad (11)$$

with $S_1 = \text{Tr}(C \cdot C^\dagger) = \sum_{n=1}^N \lambda_n$ with $S_1 = 1$ refers to unit trace constant and

$$\Lambda = N_A N_B (Y_1 - Y_0) \quad (12)$$

as the rescaled ensemble complexity parameter with $N_A N_B$ as the size of the Hilbert space in which state $|\Psi\rangle$ resides, and

$$g_1(\Lambda, S_1) \equiv \left(\frac{\langle R_0 \rangle}{N} - q_0 J \right), \quad g_2(\Lambda, S_1) \equiv -\frac{2\beta S_1}{N} \left\langle \frac{1}{S_2} \right\rangle \quad (13)$$

with $R_0 = -\sum_n \log \lambda_n$ and $S_2 = \sum_{n=1}^N \lambda_n^2$ and $q_0 = \frac{2N+\nu_0-1}{N+\nu_0}$. Here J is the normalization constant set to unity in the present work: $J \equiv J(S_1) = \int D\lambda P_c = 1$ We note, for latter reference, $g_1(\infty, 1) \approx \frac{\langle R_0(\infty, 1) \rangle}{N} \approx \log N$ and $g_2(\infty, S_1) \equiv -\frac{2\beta}{N} \left\langle \frac{1}{S_2} \right\rangle \sim \log N$ with $\langle R_1(\infty, 1) \rangle =$

$\left(\log N - \frac{N}{2(N+\nu_0)}\right)$ and $\langle R_2(\infty, 1) \rangle = \log \frac{N(N+\nu_0)}{2N+\nu_0-1}$. For brevity, large N limit of $\langle R_n(\infty, 1) \rangle$ will also be referred as $R_{n,\infty}$.

Eq.(11) can be solved by method of characteristics leading to a general solution $\langle R_n \rangle(\Lambda, S_1)$ for arbitrary trace S_1 . As our interest is in $S_1 = 1$ and for a separable initial state chosen at $Y_1 = Y_0$ i.e. $\Lambda = 0$ with $\langle R_n(0, 1) \rangle = 0$, the solution becomes (*appendix A*),

$$\langle R_n(\Lambda, 1) \rangle \approx \frac{(-1)^{n-1}}{n} g_n(\Lambda, 1) \left[1 - L^{-\tau(\frac{\beta\Lambda}{2}-1)} \right]. \quad (14)$$

Here τ is an arbitrary function independent of Λ and is introduced to ensure correct limiting behaviour for $\langle R_n \rangle$ in the limits $\Lambda \rightarrow 0$ and ∞ ; this requires $\tau \rightarrow 0$ in large N limit but $\tau\Lambda \rightarrow \infty$ if $\Lambda \rightarrow \infty$. (As discussed later in section III.B, $\tau = 1/D_n$ where D_n is defined in eq.(33)). The above exponential form for $\langle R_n \rangle$ is also supported by the solution obtained by an alternative route discussed in [15] (given by eq.(43) therein) as well as numerical analysis. (We recall that $\langle R_n(\Lambda, 1) \rangle$ theoretically predicted in [15] is of form similar to eq.(14) but with $\tau = 1$ and $g_n(\Lambda, 1)$ approximated as $R_{n,\infty}$; the latter approximation was based on ignoring the Λ -variation of $\langle R_0 \rangle(\Lambda, 1)$ with respect to $\langle R_n \rangle(\Lambda, 1)$).

Eq.(14) depends on $g_n(\Lambda, 1)$ and thereby requires information about Λ -dependence of $\langle R_0 \rangle$ and $\langle \frac{1}{S_2} \rangle$. Proceeding as in case of R_1, R_2 , the Λ dependent behaviour of $\langle R_0 \rangle$ and $\langle Q \rangle \equiv \langle \frac{1}{S_2} \rangle$ can be given as (details in *appendices B, C* respectively)

$$\langle R_0 \rangle(\Lambda, 1) = \langle R_0 \rangle(\infty, 1) + \frac{N^2}{2\gamma\tau(\Lambda - 1)} \quad (15)$$

$$\langle Q \rangle(\Lambda, 1) = e^{\tau(1-(\beta\Lambda/2))} + \frac{\beta}{2N} \langle Q^2 \rangle (1 - e^{\tau(1-(\beta\Lambda/2))}) \quad (16)$$

For brevity, a function $\langle F \rangle(\Lambda, 1)$ will hereafter be denoted as $\langle F \rangle(\Lambda)$.

C. Determination of rescaling parameter τ

The unknown τ , appearing as a rescaling parameter of Λ in eqs.(14, 15, 16), has an important role: it is introduced to satisfy the desired limiting behaviour of the function at $\Lambda = 0, \infty$. To determine τ , we proceed as follows.

We note that the first term in the right side of eq.(10) smaller by $O(N)$ as compared to others term and can be neglected in large N limit; this can be seen by a rescaling of Schmidt

eigenvalues $\lambda_n \rightarrow r_n D$, with $D \sim N^b$ ($b \sim 1$ based on numerics discussed in section III). With $P_\lambda(\lambda_1, \dots, \lambda_N) D\lambda = P_r(r_1, \dots, r_N) Dr$, eq.(10) in terms of rescaled variables becomes

$$\frac{\partial P_r}{\partial Y_1} \approx - \sum_{n=1}^N \frac{\partial}{\partial r_n} \left(\frac{1}{D} \sum_{m=1}^N \frac{\beta r_n}{r_n - r_m} - 2\gamma r_n \right) P_r \quad (17)$$

The constraint $\sum_n \lambda_n = 1$ on the eigenvalues λ_n now becomes $\sum_n r_n = \frac{1}{D}$. As clear from the above, the repulsion term contribute significantly for $D \sim \Delta^{-1}$ where Δ is the average level spacing between Schmidt eigenvalues, and, \mathcal{J} gives the normalization of JPDF P_r :

$$\mathcal{J} = \int \delta \left(\mathcal{S}_1 - \sum_k r_k \right) P_r Dr. \quad (18)$$

The choice of $J = 1$ then gives normalization constant C_{hs} for P_c as $C_{hs} = \frac{D}{\mathcal{J}}$. We also define

$$\langle \mathcal{F} \rangle = \mathcal{J}^{-1} \int \mathcal{F}(r) \delta \left(\mathcal{S}_1 - \sum_k r_k \right) P_r Dr \quad (19)$$

A substitution of $\mathcal{R}_1(r) = -\sum_k r_k \log r_n$ and $\mathcal{R}_2(r) = -\log(\sum_k r_k^2)$ in the above equation gives $\langle \mathcal{R}_1 \rangle$, $\langle \mathcal{R}_2 \rangle$ respectively. Similarly a substitution of $\mathcal{R}_0(r) = -\sum_k \log r_n$ and $\mathcal{Q}(r) = -\frac{1}{\sum_k r_n^2}$ also gives $\langle \mathcal{R}_0 \rangle$ and $\langle \mathcal{Q} \rangle$.

Using the definition in eq.(6) and $S_1 = D \mathcal{S}_1$, where $\mathcal{S}_1 \equiv \sum_n r_n$, we now have

$$\langle R_1(\Lambda, S_1) \rangle = D \langle \mathcal{R}_1(\Lambda, \mathcal{S}_1) \rangle - \log D \quad (20)$$

$$\langle R_2(\Lambda, S_1) \rangle = \langle \mathcal{R}_2(\Lambda, \mathcal{S}_1) \rangle - 2 \log D \quad (21)$$

Similarly

$$\langle R_0(\Lambda, S_1) \rangle = \langle \mathcal{R}_0(\Lambda, \mathcal{S}_1) \rangle - N \log D \quad (22)$$

$$\langle Q(\Lambda, S_1) \rangle = \frac{\langle \mathcal{Q}(\Lambda, \mathcal{S}_1) \rangle}{D^2} \quad (23)$$

As given by eq.(D5) in *appendix D*, the mathematical forms of \mathcal{R}_n satisfying required boundary conditions can be determined without any unknowns. A substitution of eq.(D5) in eq.(20) gives

$$\langle R_1(\Lambda, 1) \rangle = \frac{\langle R_0 \rangle}{N} \left(1 - L_A^{\left(\frac{1}{D} - \frac{\chi_1 \beta \Lambda}{2D} \right)} \right) \quad (24)$$

Similarly substitution of eq.(D5) in eq.(21) gives

$$\langle R_2(\Lambda, 1) \rangle = \frac{\chi_2}{\chi_1} \frac{4\langle Q \rangle}{\beta N} \left(1 - L_A^{\left(\frac{\chi_2}{\chi_1^D} - \frac{\chi_2 \beta \Lambda}{2D} \right)} \right) \quad (25)$$

with $\chi_1 = \frac{N+2\nu D-1}{N+2\nu-1}$, $\chi_2 = \frac{N+\nu D-1}{N+2\nu-1}$. With $\nu = (N_B - N_A + 1)/2$ and $N_A = N$, we note that χ_1, χ_2 become significant for cases with $N_B \gg N_A$.

In large N -limit, and for cases with $\chi_2 \sim \chi_1$, eq.(24) and eq.(25) can further be approximated as

$$\langle R_n(\Lambda) \rangle \approx \frac{(-1)^{n-1}}{n} g_n(\Lambda) (1 - L_A^{-\frac{\beta \Lambda}{2Dn}}) \quad n = 1, 2 \quad (26)$$

where $g_n(\Lambda)$ is given by eq.(13) (with $\langle R_0 \rangle$ and $\langle Q \rangle$ by eq.(15) and eq.(16) respectively) and $D_n = \frac{D}{\chi_n}$.

Intuitively the rescaling of Λ in eq.(32) can be explained as follows: $\langle R_n(\Lambda) \rangle$ is a function of Schmidt eigenvalues $\lambda_1, \dots, \lambda_N$ of the matrix $C \cdot C^\dagger$. While in separability limit, a typical eigenvalue is zero (with only one of them equal to 1), it is $\sim 1/N$ in maximum entanglement limit or the ergodic limit of the ensemble (stationary Wishart limit). Further the typical mean level spacing between eigenvalues in the former limit is 0, it is $1/N$ in the latter limit. Based on the second order perturbation theory of the eigenvalues of Hermitian matrices, a change from one limit to the other is therefore expected to take place for $(Y_1 - Y_0) \sim o(1/N)$ (i.e., the parameter value at which the repulsion becomes significant enough). The appropriate parameter governing the evolution in this regime is therefore $\sim N(Y_1 - Y_0)$ equivalently Λ/D . (As confirmed by numerics too, the entropy shows a rapid change in the regime $Y_1 - Y_0 \sim 1/N$). Indeed this is equivalent to a rescaling of the Schmidt eigenvalues so as to capture the contribution from the eigenvalue repulsion term in eq.(10) to $\langle R_n \rangle$.

D. Role of constants of evolution

The theoretical study in [15] indicated that the evolutionary paths for $\langle R_n \rangle(\Lambda)$ for different ensembles, with initial condition as a separable state for each of them, are governed by a single parameter Λ but did not elaborate on the role of the constants Y_2, \dots, Y_M . The numerical study in [15] however indicated almost analogy of the evolutionary paths in terms

of Λ (an almost collapse onto the same curve in terms of Λ) thus implying either no role of constants or same constants for all ensembles considered for numerics. The results in [15] were however based on small- N numerics, and for balanced condition $N_A = N_B = N$. As the previous study left many queries left unanswered, it is relevant to pursue a detailed numerical analysis in large N_A limit and verify the improved theoretical prediction given by eq.(14).

The transformation $\{h_{kl}, b_{kl}\} \rightarrow Y_1, \dots, Y_M$ also implies the transformation of the ensemble density in eq.(1) to $\rho(C; Y_1, \dots, Y_M)$. The ensembles with different sets of $\{h_{kl}, b_{kl}\}$ can have different values of Y_1, \dots, Y_M , the transformed ensemble density is therefore represented by different points in complexity parameter space.

In general different states will evolve along different paths in Y -space. It is however possible that two different Gaussian states, represented in two different basis, still have same sets of constants Y_2, \dots, Y_M for both of them. Such states will evolve, with Y_1 as the evolution parameter, along same path in Y -space but that does not ensure same entanglement entropy for them. As discussed in section III, the latter requires analogy of a rescaled Y_1 .

A relevant query in the above context is whether the constants of evolution Y_2, \dots, Y_M can always be chosen same for a set of states represented by eq.(1) if they are subjected to same set of global constraints e.g symmetry and conservation laws? Intuitively the answer is in affirmative and can be justified as follows: a physically motivated basis to represent a state is usually based on its global constraints. Different states with a common set of global constraints can then be represented in same/ equivalent basis. A typical matrix in general has many basis constants [28] which can then be chosen as the constants of evolution Y_2, \dots, Y_M . This is later explained through three simple examples (section III.A).

Eq.(26) suggest a deep universality underlying the pure states represented by the multi-parametric Gaussian ensembles. This can be elucidated as follows. Different states are in general represented by different ensemble parameters ($\{h, b\}$ sets) in eq.(7) and a variation of these parameters is in general expected to lead to their different evolutions. But, following from eq.(26), the evolution is not governed by the details of $\{h, b\}$ sets but only by a specific function $\Lambda_{ent}(\{h, b\}, N_A)$ and a set of constants of evolution Y_2, \dots, Y_M . In general, if the latter are different, notwithstanding same Λ_{ent} for the two states, the paths of their evolution are expected to differ. But, as explained above, the latter can be chosen as the functions of basis constants. As a matrix has a large number of basis constants, the constants Y_2, \dots, Y_M

can be chosen same for different ensembles represented in a fixed basis [28]. This in turn leaves the evolution characterized only by Λ_{ent} . At some intermediate stage of evolution, it may happen that two different states (i.e., represented by different $\{h, b\}$ sets in eq.(7)) may correspond to same Λ_{ent} value; Eq.(26) then predicts their entanglement entropies to be equal at that point if their constants of evolution are also same. More clearly, different states with same Λ_{ent} value are predicted to share same entanglement entropy, irrespective of the details about their $\{h, b\}$ sets and therefore form a universality class characterized by Λ_{ent} . As for finite N , the latter can vary continuously between $0 \rightarrow \infty$, the above predicts infinite number of universality classes of the entanglement statistics among pure Gaussian states characterized by Λ_{ent} .

Any change in system conditions with time however may change the system parameters and thereby the state. This in turn is expected to reflect on the parameters of the state matrix ensemble (if it is a suitable representation of the state). Consequently the two evolving states need not retain the analogy of Y_1 and thereby Λ_{ent} afterwards.

We emphasize that the universality reported here is different and indeed much deeper from the one discussed previously, e.g., for excited states [29], ground states [17, 30–37], correspondence between criticality and logarithmic entanglement entropy scaling [17, 38–42], states with topological properties [18, 43, 44], etc.

III. NUMERICAL ANALYSIS

Our primary focus in this work is to numerically analyse the states with Gaussian distributed components and seek (i) the validity of eq.(14), i.e, whether a universality of entanglement entropy can be achieved for the state matrix ensembles described by eq.(1) with different sets of h_{kl}, b_{kl} in eq.(7), (ii) a search for a critical regime in which the entanglement entropy of a non-ergodic state does not change with system size, (iii) the sub-system size scaling of the entanglement entropy for a fixed complexity parameter and to understand robustness of universality to sub system-size variation,

A. Details of the ensembles

To verify the above claims, we consider four different ensembles with independent Gaussian distributed matrix elements with zero mean but different decaying-types of variances; the latter imply different decay rates for the typical correlations between two orthogonal subspaces of the bipartite state. The specific details for each ensemble can be given as follows (noting that the row index refers to orthogonal base of subsystem A and the column index to that of B).

Brownian ensemble (BE): with variance $h_{k1} = 1, l = 1$; $h_{kl} = (1 + \mu)^{-1}, l > 1$ and mean $b_{kl;s} = 0 (\forall k, l)$ in Eqn. (7), typically we have $C_{kl} \sim (1 + \mu)^{-1/2}$ for $l > 1$ in this case. The latter describes a state with typically same order of overlap between basis state pairs of A with B except for pairs $|a_k b_l\rangle$. With initial ensemble chosen with $\mu \rightarrow \infty$, Eqn. (12) gives

$$\Lambda = -\frac{N_A(N_B - 1)}{2\gamma} \ln \left(1 - \frac{2\gamma}{(1 + \mu)} \right). \quad (27)$$

Power law decay ensembles (PE): with $h_{kl} = \left(1 + \frac{k(l-1)}{\mu}\right)^{-1}$, $b_{kl} = 0 \quad \forall k, l$, C_{kl} here typically decays as a power law along rows as well as columns. Contrary to BE case, this implies a variation of typical contributions from the basis state-pairs $|a_k\rangle |b_l\rangle$ for $k \neq l$. With initial ensemble parameter $\mu \rightarrow 0$, Eqn. (12) gives

$$\Lambda = -\frac{1}{2\gamma} \sum_{r_1=1}^{N_A} \sum_{r_2=1}^{N_B-1} \ln \left(1 - \frac{2\gamma}{1 + \frac{r_1 r_2}{\mu}} \right) \quad (28)$$

Exponential decay ensemble (EE): with $h_{kl} = \exp\left(-\frac{k|l-1|}{\mu}\right)$, $b_{kl} = 0 \quad \forall k, l$; this case is similar to that of PE except for an exponential decay of C_{kl} for sub-bases pairs with higher indices. Here again with initial ensemble parameter $\mu \rightarrow 0$, Eqn. (12) gives

$$\Lambda = -\frac{1}{2\gamma} \sum_{r_1=1}^{N_A} \sum_{r_2=1}^{N_B-1} \ln \left[1 - 2\gamma \exp\left(-\frac{r_1 r_2}{\mu}\right) \right]. \quad (29)$$

Sparse Ensemble (SE): Contrary to previous three ensembles, some of the matrix elements in this case are exactly zero, with sparsity decreasing as n increases. Here again

we choose $b_{kl} = 0$ for all entries, and,

$$h_{kl} = \begin{cases} \exp \left[- \left(\frac{k(l-1)}{w^2} \right) \right] & d(k, l) = 0, \\ \exp \left[- \left(\frac{k(l-1)}{w_s^2} \right) \right] & 0 < d(k, l) \leq n, \end{cases} \quad (30)$$

where, $d(k, l)$ is the *hamming distance* between the bases k and l , defined as the number of bit flips required to make $k = l$, which has a practical significance to quantum error correction [45]. In contrast to the ensembles mentioned above, this case has more free parameters: w , w_s , and n . The initial ensemble in this case corresponds to the choice $w, w_s \rightarrow 0$ which gives

$$\Lambda = -\frac{1}{2\gamma} \left[\sum_{r=1}^{N_A} \ln \left(1 - 2\gamma \exp \left(-\frac{r(r-1)}{w^2} \right) \right) + \sum_{r_1, r_2} \ln \left(1 - 2\gamma \exp \left(-\frac{r_1(r_2-1)}{w_s^2} \right) \right) \right], \quad (31)$$

where \sum_{r_1, r_2} is over r_1 and r_2 satisfying $0 < d(r_1, r_2) \leq n$.

We note that each ensemble mentioned above correspond to zero centred Gaussian entries; the latter implies the typical values of the components of the state (i.e., typical entries in a typical state matrix of the ensemble) of the order of variance. Further BE, PE and EE are same as used in our previous study [15] of entanglement entropy with an important difference: previously the subsystem sizes N_A, N_B were kept fixed with only parameter μ varying. In the present analysis, c, α and N_A act as free parameters ($\mu \equiv c N_A^\alpha$; see section III C), thereby facilitating the analysis of subsystem size effect on the universality of the evolutionary path from separability to maximum entanglement. The choice of the same ensembles helps us in a direct comparison with our previous results too.

Another point worth noting is the choice of the initial ensemble for the evolution: in each case it corresponds to an ensemble of matrices C with non-zero elements (distributed as zero centred Gaussians and typically of the order of the variance) only in the first column, i.e., $C_{kl} = 0$ if $l \neq 1$. A typical matrix $C \cdot C^\dagger$ in the initial ensemble corresponds to zero entanglement in following sense: as variances of the higher columns also go to zero (except first one), this leaves state matrix as rank one and therefore state as separable: $\Psi = \sum_k C_{k1} |a_k\rangle |b_1\rangle$. While a separable state can be represented by alternative C matrix-forms, the one mentioned above however has an additional advantage: with initial state chosen in the above form, the evolution of entanglement manifests directly through the increase in elements in higher columns, with almost all columns becoming of the same order in maximum entanglement limit.

As mentioned in section II, the parameter γ corresponds to the variance of the matrix elements of the ensemble at the end of crossover. For the ensembles mentioned above, the Wishart limit is reached as $h_{kl} \approx h_{kk} = 1$. This gives $\gamma = 1$ for our numerical analysis of the evolution.

As mentioned above, the condition $\frac{\partial \rho}{\partial Y_\alpha} = 0$ for $\alpha > 1$, implies Y_α as the constants of evolutions; the latter can be determined by solving the characteristic equation (for the case $b_{kl;s} \neq 0$) $\frac{dh_{kk;s}}{2(1-\gamma h_{kl;s})} = \dots = \frac{dh_{kl;s}}{2(1-\gamma h_{kl;s})} = \frac{db_{kl;s}}{\gamma b_{kl;s}} = \frac{dY_\alpha}{0}$. A general solution of the above equation is $F(Y_\alpha, \alpha_1, \dots, \alpha_{M-1}) = 0$ where α_n are the constant surfaces obtained by solving the above set of M differentials. For example, for the matrix of mean values $b = \{b_{kl;s}\} = 0$, the choice of an arbitrary pair of differentials gives $\frac{dh_{mn;s}}{1-\gamma h_{mn;s}} = \frac{dh_{ij;s}}{1-\gamma h_{ij;s}}$ with the corresponding solution as $\log\left(\frac{1-\gamma h_{mn;s}}{1-\gamma h_{ij;s}}\right) = \text{constant}$; the constant so obtained can then be chosen as one of the Y_α 's for $\alpha > 1$. Indeed, for BE, the above condition can be satisfied by any two pairs of indices m, n and i, j giving $\log\left(\frac{1-\gamma h_{mn;s}}{1-\gamma h_{ij;s}}\right) = 0$; as many such pairs can be formed, we have $Y_\alpha = \left(\frac{1-\gamma h_{mn;s}}{1-\gamma h_{ij;s}}\right) = 1$ for all $\alpha > 1$. For PE and EE, the condition is satisfied by a specific combination of pairs, i.e., m, n and $n-1, m+1$: $d\log(1-\gamma h_{mn;s}) - d\log(1-\gamma h_{n-1, m+1;s}) = 0$ giving $\log\left(\frac{1-\gamma h_{n-1, m+1;s}}{1-\gamma h_{mn;s}}\right) = 0$; Y_k can then be chosen as $Y_\alpha = \frac{1-\gamma h_{n-1, m+1;s}}{1-\gamma h_{mn;s}} = 1$. Proceeding similarly in SE case, pairs of $h_{mn;s}$ can be identified which lead to $Y_k = 1$. As the above indicates, it is possible to choose same set of constants Y_α for BE, PE and EE, namely $Y_\alpha = 1$.

We note that the existence of a solution of the type mentioned above requires $h_{mn;s} \propto h_{ij;s}$ (satisfied by all pairs in BE case and for specific pairs in PE and EE case) and need not exist for all ensembles. The alternative solutions leading to constants Y_α can then be obtained, e.g., by considering combinations of more than a pair of differentials (e.g $dY_\alpha \equiv \sum_{mn;s} \frac{q_{mn;s} dh_{mn;s}}{1-\gamma h_{mn;s}} = 0$ with $\sum_{mn;s} q_{mn;s} = 0$ with $q_{mn;s}$ arbitrary functions). Indeed as indicated by the study [28], a matrix of $N \times N$ has many basis constants which can be chosen as the constants of evolution Y_α ; this implies that the transformation $h, b \rightarrow Y$ -space can always be defined for a given basis.

B. Universality of evolutionary route

A bipartite quantum state represented by ρ_{cn} (eq.(1)) with ρ_c given by eq.(7) corresponds to a point in h, b -space. The $\{h, b\} \rightarrow Y$ -space mapping gives the location of the state in

Y-space, labelled by Y_1, \dots, Y_M . Due to any change in system conditions, different state ensembles and thereby their entanglement entropies $\langle R_n \rangle$ would then evolve along different invariant curves (in M -dimensional space with $M - 1$ invariants) marked by the corresponding set of constants Y_2, \dots, Y_M . (The different ensembles in this paper only refer to those with different means and variances in eq.(7).) The paths of evolution however would be analogous if the constants of evolutions are same for all ensembles under consideration. The entanglement entropies of two such ensembles, say “1” and “2” would also be same if $\Lambda_{ent,1} = \Lambda_{ent,2}$.

In [15], We compared $\langle R_1 \rangle$ and $\langle R_2 \rangle$ numerically for each one of the three ensembles mentioned above and found an analogous evolution of the two entropies in terms of the parameter Λ_{ent} for “balanced condition” $N_A = N_B$. The analogy was consistent with our theoretical prediction in [15] with $g_n \approx R_{n,\infty}$ and $\tau = 1$; here the notation $R_{n,\infty}$ implies $\lim_{\Lambda \rightarrow \infty} \langle R_n \rangle(\Lambda)$. This was indeed expected as the constants of evolution are same for both entropies of a given ensemble and $R_{1,\infty} = R_{2,\infty}$.

The study [15] also suggested that the evolutionary paths for $\langle R_n \rangle$ for different ensembles, with initial condition as a separable state for each of them, are almost analogous in terms of Λ . The study was however based on small- N numerics as well as balanced condition $N_A = N_B = N$ and indicated only an almost collapse onto the same curve in terms of Λ . We pursue the investigation further in the present study by a numerical comparison of the dynamics of $\langle R_1 \rangle$ and $\langle R_2 \rangle$ for large size ensembles and for unbalanced condition $N_A \neq N_B$. Here $N_A = q^{L_A}$ with q as the size of the local Hilbert space (i.e., the one for a basic unit of which subsystems A and B consist of). For clarity of presentation, here we consider the basic units as the qubits, thus implying $q = 2$. For numerical analysis, the Schmidt eigenvalues are derived by an exact diagonalization of the ensembles of $N_A \times N_A$ matrices $W = C \cdot C^\dagger$, with C taken from a BE, PE, EE or SE. Invoking the relation $R_1 = -\sum_{k=1}^{N_A} \lambda_k \log \lambda_k$ and $R_2 = -\log \left(\sum_{k=1}^{N_A} \lambda_k^2 \right)$ now gives R_1 and R_2 for each matrix; the average over an ensemble for fixed ensemble parameters then leads to $\langle R_1 \rangle(\Lambda), \langle R_2 \rangle(\Lambda)$ for a given Λ -value. Repeating the procedure for each ensemble for many values of the ensemble parameters thereby leads to the results describing evolution of $\langle R_n \rangle$ as a function of Λ ; the above procedure is later referred as the *numerical diagonalization route*. As shown in Fig. 1 for each case (with L_A fixed), we find the analogy only if Λ is further rescaled by an ensemble specific parameter

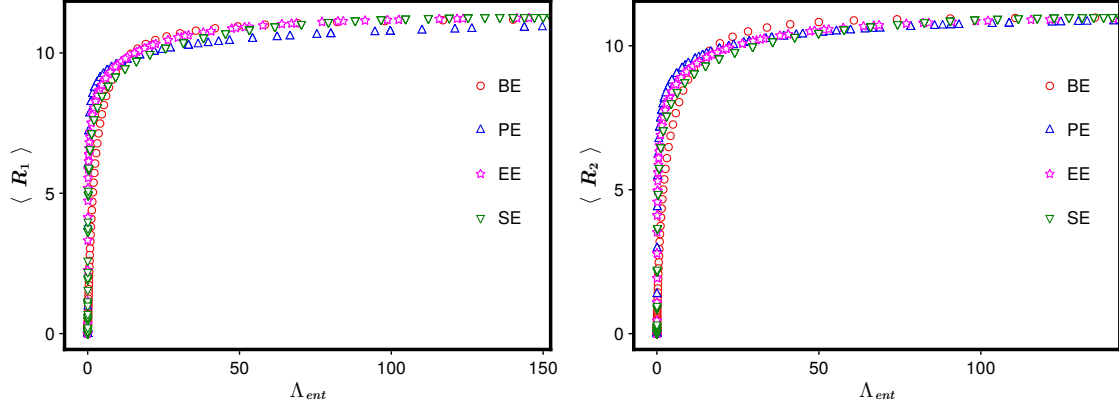


FIG. 1: Comparison of entanglement dynamics for various ensembles, *e.g.*, ensemble whose variance is constant (BE) Eqn. (27), decays as power-law (PE) Eqn. (28), decays exponentially (EE) Eqn. (29), with respect to the first column, and the sparse ensemble (SE) Eqn. (31) is shown for (a) $\langle R_1 \rangle$ and (b) $\langle R_2 \rangle$, with the *complexity-parameter* (Λ) rescaled with the respective parameters D_1 and D_2 . The partition in this case is balanced, and the parameter D_1 and D_2 for BE, PE, EE and SE for both the measures can be interpolated from figs. 2 for $L_A = 12$.

(D_n) leading to

$$\Lambda_{ent} = \frac{\Lambda}{D_n}. \quad (32)$$

To gain insight in the ensemble-dependence of D_n , we numerically analyse $\langle R_n(\Lambda) \rangle$ for the four ensembles for all possible bipartitions (i.e., for a fixed system size L but varying subsystem size L_A) and extract D_n values by fitting to Eqn. (14). Based on numerical insights, we conjecture

$$D_{1,2}(N_A) = a N_A^b = a 2^{bL_A} \quad (33)$$

with $b \sim 1$ and a dependent on the nature of the ensemble *e.g.*, nature of the decay of the higher column variances (with respect to first one). The numerical data obtained from four different ensembles, displayed in figs. 2 supports the above conjecture (more discussion in next section). Further the numerical insight about universality in terms of a rescaled Λ (eq.(32)) is consistent with eq.(26).

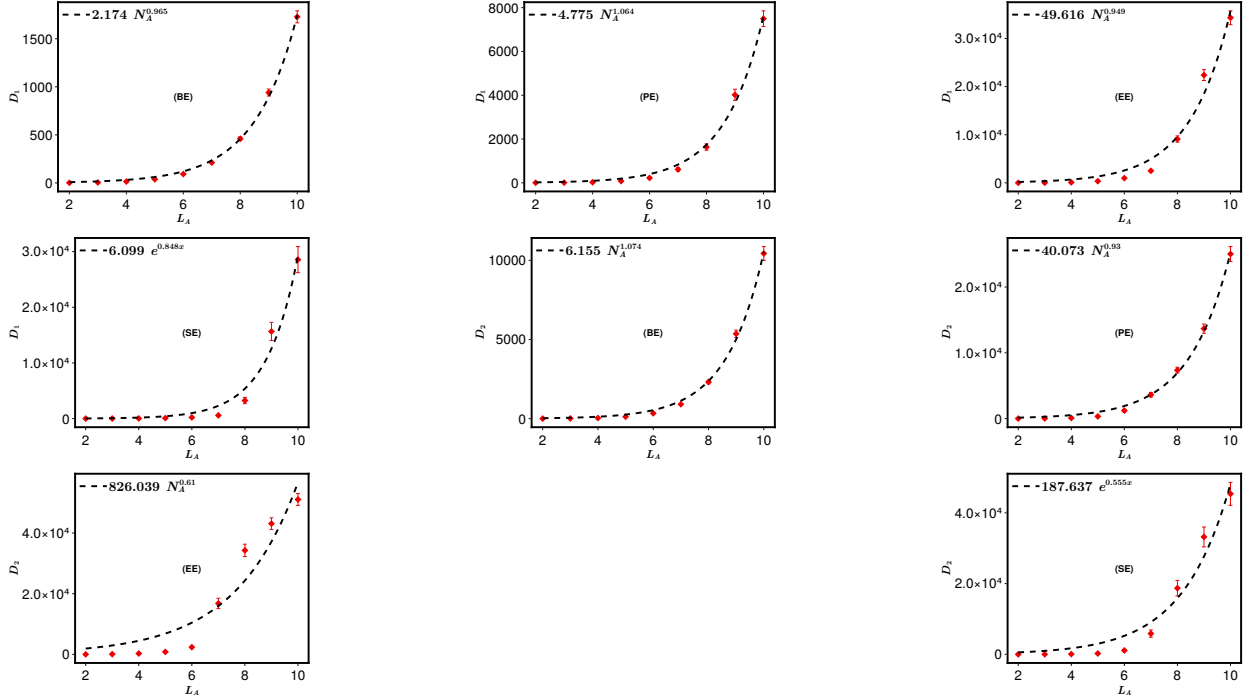


FIG. 2: D_1 and D_2 are numerically obtained as a function of sub-system size (L_A) for the three different ensembles: BE, PE, EE and SE from (a)-(d) respectively for R_1 and (e)-(h) for R_2 . We analyse the entanglement dynamics for various “cut” and later fit the analytic form Eqn. (26) for R_1 and R_2 . We find D_n scaling exponentially with the sub-system size to be the optimum fit, whose goodness has been quantified by its R^2 value. The function, along with the fit parameters, is shown in the legend ($N_A = 2^{L_A}$).

C. Finite Size Scaling and Criticality of the entanglement

For clarity of presentation, here we consider R_1 only and for equal subsystem sizes $N_A = N_B = 2^{L_A} = 2^{L_B}$ i.e. balanced condition $L_A = L_B$ (with $L_A = \log_2 N_A$).

Based on previous studies, R_1 for a generic state of a one dimensional system is believed to scale with subsystem size L_A as

$$R_1 = q_1 L_A + q_2 \log L_A + \text{constant} \quad (34)$$

with q_1, q_2 as constants. Typically, $q_1 \neq 0, q_2 = 0$ for ergodic states [29, 46], while $q_1, q_2 = 0$ for some non-ergodic states and $q_1 = 0, q_2 \neq 0$ for states in critical regime [47].

It is natural to query whether a similar behaviour can be seen for R_1 averaged over the ensembles of states given by eq.(1). Eqn. (26) for the latter implies

- (i) $\langle R_1(\Lambda) \rangle \rightarrow L_A$ and thereby approaching volume law for $\Lambda \gg D_1$ and in large L_A limit,
- (ii) $\langle R_1(\Lambda) \rangle \rightarrow 0$ and thereby approaching separability for $\Lambda \ll D_1$,
- (iii) For $\Lambda \sim \frac{D_1}{\log L_A}$, however, the critical behaviour can result if $g_1(\Lambda)$ and $L^{-\Lambda/D_1}$ conspire together to give $\langle R_1 \rangle \sim \log L_A$ with $g_1(\Lambda) \approx \langle R_0 \rangle(\Lambda)/N$. From eq.(15), $\langle R_0 \rangle(\Lambda)$ in this can be approximated by $\langle R_0(\infty) \rangle$.

Further, with both Λ and D_1 dependent on L_A , the above suggests a L_A -scaling of $\langle R_1 \rangle$ near the critical point $\Lambda_{ent}^* = \frac{\Lambda^*}{D_1}$. To verify this aspect, we apply a finite size scaling approach as follows. Assuming $\Lambda = \Lambda(\alpha L_A)$, $\Lambda^* = \Lambda(\alpha^* L_A)$ as its value at the critical point Λ_{ent}^* and α as a variable used for scaling analysis, we write $\langle R_1(\Lambda_{ent}) \rangle$ a function of the scaling variable $(\alpha - \alpha^*)L_A^{\frac{1}{\nu}}$,

$$\langle R_1(\Lambda_{ent}) \rangle = F((\alpha - \alpha^*)L_A^{1/\nu}) \quad (35)$$

with α^* as the critical point of the transition in $\langle R_1(\Lambda_{ent}) \rangle$ with a critical exponent ν and $F(x)$ as an arbitrary function of x . To analyse the scaling of $\langle R_1(\Lambda_{ent}) \rangle$ near the critical point α^* , we consider Eqn. (35) with $\langle R_n(\Lambda_{ent}^*) \rangle = F(0)$.

In order to seek the scaling behaviour and whether a critical ensemble parameter α^* can indeed exist for the non-ergodic states represented by eq.(1), we consider two routes: (i) the *numerical diagonalization route* mentioned in section III B, and, (ii) as $\langle R_1 \rangle$ is theoretically predicted by Eqn. (26), it is natural to query whether it displays the same scaling behaviour as by the previous route (referred below as *theory route*). We note that our critical point analysis here is confined to BE, PE and EE only with required Λ_{ent} obtained from Eqn.(32) along with Eqn.(27, 28, 29) for Λ and Eqn.(33) for D_1 . Indeed the determination of the critical parametric value for SE requires a separate analysis, without providing any additional insights.

For BE, we consider the case with $\mu = c_1 N_A^\alpha = c_1 2^{\alpha L_A}$ with c_1 a non-zero, finite constant; Eqn. (27) gives

$$\Lambda = c 2^{(2-\alpha)L_A}. \quad (36)$$

with $c = 1/c_1$. For PE and EE with $\mu = c_1 N_A^{2-\alpha} = c_1 2^{(2-\alpha)L_A}$, Eqn. (28) and Eqn. (29) again give eq.(36) but now $c = c_1 H_{N_A} H_{N_B-1}$, for PE with H_N as the N^{th} Harmonic number, and, $c = c_1 \Gamma[0, (c_1 2^{(2-\alpha^*)L_A})^{-1}]$ for EE, with $\Gamma(a, x)$ as the incomplete Gamma function. Eqn.(36) then gives $\Lambda^* = c 2^{(2-\alpha^*)L_A}$, this along with Eqn. (32) and Eqn.(33) give Λ_{ent} -value

at the critical point as $\Lambda_{ent}^* = \frac{\Lambda^*}{D_n} = \frac{c}{a} 2^{(2-b-\alpha^*)L_A}$. We note that while c for BE is a constant, c for PE and EE retains, albeit weak, dependence on L_A .

Eq.(32) along with eq.(36) gives $\Lambda_{ent} = \frac{c}{a} 2^{(2-b-\alpha)L_A} = 2^{(\alpha^*-\alpha)L_A} \Lambda_{ent}^*$. For $\alpha > \alpha^*$, $\lim_{L_A \rightarrow \infty} \Lambda_{ent} \rightarrow 0$, $\langle R_1 \rangle \rightarrow 0$; from eq.(26), the state is therefore expected to approach the separability limit. For $\alpha < \alpha^*$, $\lim_{L_A \rightarrow \infty} \Lambda_{ent} \rightarrow \infty$, $\langle R_1 \rangle \rightarrow \frac{\langle R_0(\infty) \rangle}{N} \approx L_A$ and the state therefore approaches the maximum entanglement limit. To seek the critical value α^* , we analyse α -dependence of $\langle R_1 \rangle$ for the BE, PE and EE cases for a fixed value of c_1 (ref. Table I for details). The results for each ensemble, obtained by numerical as well as theoretical route, are displayed in Fig. 3, 4, 5 respectively. Here the required theoretical value for $\langle R_0(\Lambda_{ent}^*) \rangle$ to plot theoretical prediction in eq.(14) is determined by eq.(15). As the figures indicate, $\langle R_1 \rangle$ vs α curves for different L_A values indeed intersect each other at a common point. The corresponding scaling behaviour using $\langle R_1(\Lambda_{ent}^*) \rangle = F(0)$ are also displayed in these figures (with the left displaying theoretical and the right numerical results). As can be seen from the figures, $\langle R_1 \rangle$ behaves as a sigmoid function of $(\alpha - \alpha^*) L_A^{\frac{1}{\nu}}$. (We note that, in large N limit, eq.(26) can be approximated by a sigmoid form $\langle R_1 \rangle \approx \frac{g_1 e^x}{1+e^x}$ with $x = \Lambda_{ent}^* \log L_A$; the latter form is also consistent by the displays in the right parts of Figs.3, 4, 5. Table I displays the values of α^* , ν and $R^* \equiv \langle R_1(\Lambda_{ent}^*) \rangle$ as well as a, b for each ensemble (for arbitrarily chosen μ , equivalently c -value). A small difference between the critical values obtained from the two routes in Figs. 3 - 5 can be attributed to numerical errors in estimation of Schmidt eigenvalues through exact diagonalization as well as D_n ; we recall that the latter is again a numerical prediction.

In general, the above suggests a classification of the non-ergodic states described by Eqn. (7) in three main classes as $L_A \rightarrow \infty$: maximum entanglement, separability, and the third a critical regime with $\langle R_1 \rangle \propto \log L_A$. Based on BE, PE and EE analysis, we find that the critical behaviour $\langle R_1 \rangle \sim \log L_A$ occurs only for a specific scaling of Λ with D_1 . Based on eq.(26), this is expected to be valid for any ensemble described by eq.(7). As both Λ as well as D_1 depend on a combination of the ensemble parameters, a search for the appropriate combinations leading to critical behaviour for the SE case is technically time consuming; we expect to pursue it as a separate analysis.

For further insight, it is instructive to rewrite Eqn. (35) as $\langle R_1 \rangle = F\left(\left(\frac{L_A}{\xi}\right)^{\frac{1}{\nu}}\right)$ with $\xi = |\alpha - \alpha^*|^{-\nu}$ (for $\nu > 0$). We note that ξ has a role in separability \rightarrow entanglement transition akin to that of a wavefunction correlation length in localization \rightarrow delocalization

Ensemble	Variance (h_{kl})	D_1		D_2		c	Theory			Numerics		
		a	b	a	b		R^*	α^*	ν	R^*	α^*	ν
BE	$\begin{cases} 1, l = 1 \\ \frac{1}{1+\mu}, l \neq 1 \end{cases}$	2.174	0.965	6.155	1.074	0.1	7	1.373	0.531	6.5	1.305	0.543
PE	$\frac{1}{1 + \frac{k(l-1)}{\mu}}$	4.775	1.064	40.073	0.93	1	4.75	1.441	0.565	5	1.515	0.504
EE	$\exp \left[- \left(\frac{k(l-1)}{\mu} \right)^2 \right]$	49.616	0.949	826.039	0.61	7	2.4	1.363	0.565	4.2	1.387	0.619

TABLE I: Here, $\mu = c N_A^\alpha$, with c given in the seventh column above for each of the ensembles and $N_A = 2^{L_A}$.

transition (e.g. similar to metal \rightarrow insulator transition, ξ diverges at $\alpha = \alpha^*$); this motivates us to refer ξ as the *entanglement length*. Further, as α refers to an ensemble parameter reflecting complexity of bipartite correlations in the quantum state, and, as the ensemble represents a quantum state with maximum entanglement for $\alpha < \alpha^*$, separability for $\alpha > \alpha^*$ and a critical statistics at $\alpha = \alpha^*$, we refer α^* as marking the *edge of entanglement*.

The analysis presented above describes the search for the critical point of $\langle R_1 \rangle$. Following similar steps, the critical point of $\langle R_2 \rangle$ can also be identified; the analysis is omitted here as it does not give any new insights about critical statistics.

D. Universality and role of “cut” of Bipartition (relative subsystem size)

Previous section analysed the role of Λ_{ent} in entanglement entropy growth under “balanced constraint” on subsystem sizes i.e., $L_A = L_B$: section III B confirmed the universality of the growth in terms of Λ_{ent} for different ensembles if their constants of evolutions have

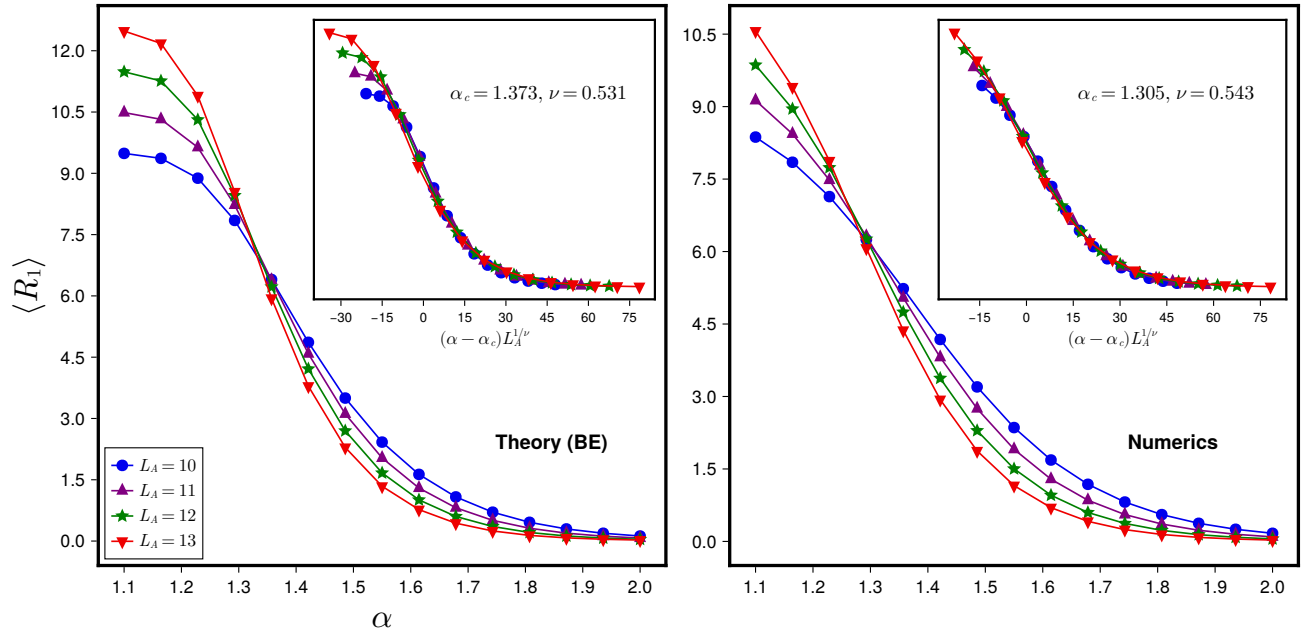


FIG. 3: (Right) The scaling of $\langle R_1 \rangle$ with α for different sub-system sizes $L_A = L/2$, for $L = 20, 22, 24, 26$ using the exact diagonalization route is shown, with a scaling collapse, using finite-size scaling, shown in the inset for BE. (Left) Eq. (26) is plotted for a theoretical comparison. The critical point (α^*) and exponent (ν) for each ensemble are also displayed in the figures. A close analogy between theory and numerics can also be observed. Similar results for PE and EE are also shown in figs. 4 and 5 respectively.

same values and have statistically analogous initial condition, and, section III C established Λ_{ent} as the parameter to characterize criticality.

With L_A a system parameter too, it is natural to query as to how the entanglement entropies evolve if the balanced constraint is removed and L_A is varied while keeping total system size $L = L_A + L_B$ as well as Λ fixed? We note that Λ_{ent} still changes due to variation of D_n with L_A and therefore $\langle R_n \rangle$ is expected to vary too. But, from Eqn.(33), D_n depends on the ensemble specific constants a, b . It is therefore not obvious whether an analogous evolutionary path of entanglement entropy, with L_A as the governing parameter, can still exist for ensembles with same Λ as well as constants of evolution?

To seek the answer, we numerically analyse the evolution of $\langle R_1 \rangle$ and $\langle R_2 \rangle$ for BE, PE, EE and SE as the “cut” of the bi-partition, i.e., L_A is varied at different fixed levels of complexity quantified by Λ (again using *numerical diagonalization route* mentioned in

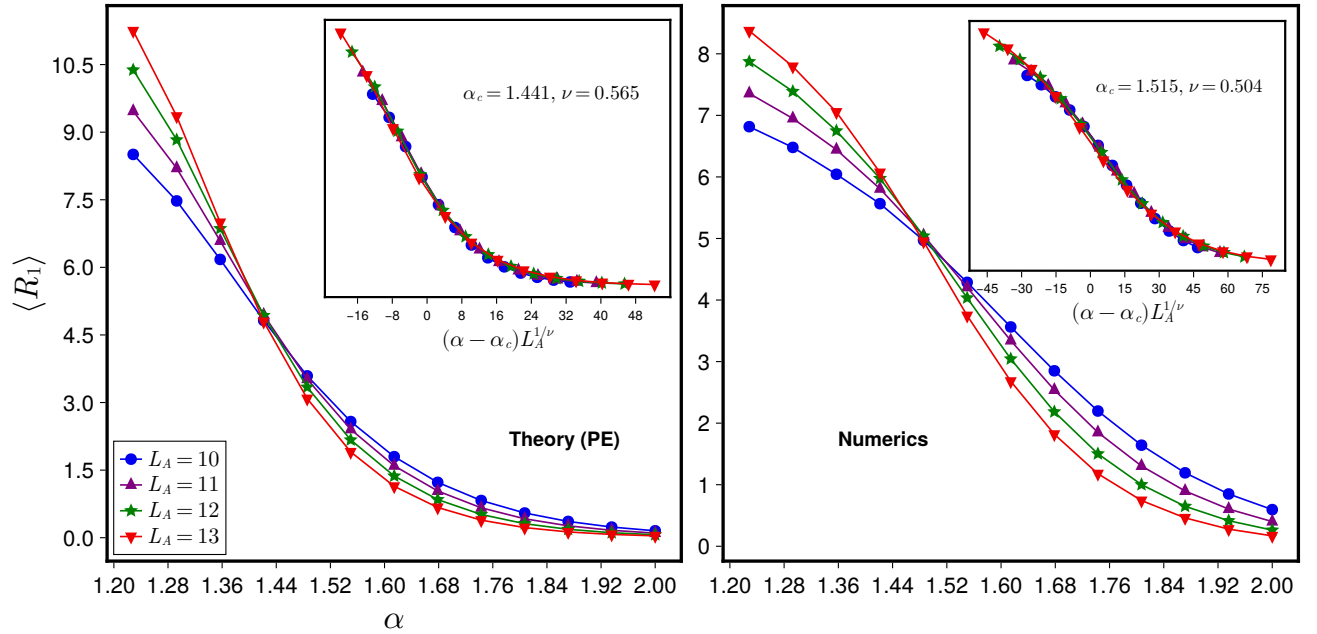


FIG. 4: The calculations as in fig. 3 is repeated here for the PE.

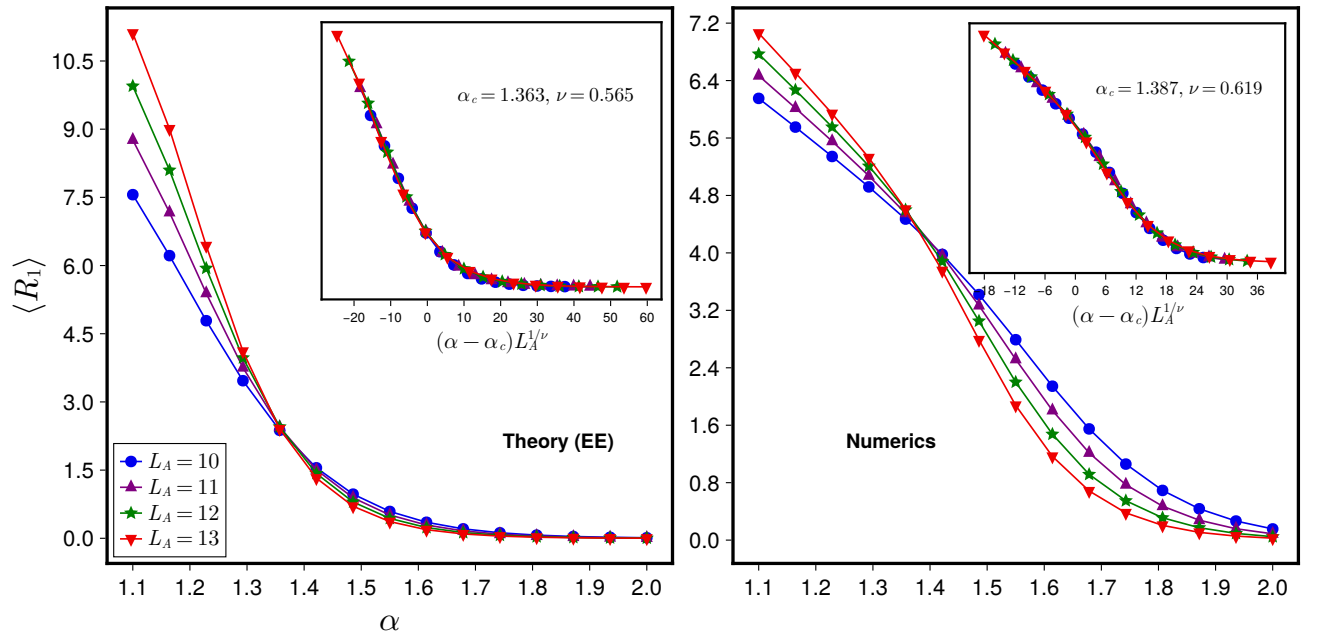


FIG. 5: The calculations as in figs. 3 and 4 is repeated here for the EE.

section III B). Here a fixed Λ for each ensemble is obtained by invoking following condition

$$\Lambda = \Lambda_{BE} = \Lambda_{PE} = \Lambda_{EE} = \Lambda_{SE} \quad (37)$$

Following from eq.(27), eq.(28), eq.(29) and eq.(31), this leads to

$$\Lambda = c_b 2^{(L-\alpha_b L_A)} = c_p 2^{(L-\alpha_p L_A)} = c_e 2^{(L-\alpha_e L_A)} = \Lambda_{SE} \quad (38)$$

with c_b, c_p, c_e and $\alpha_b, \alpha_p, \alpha_e$ as specific c and α values for BE, PE and EE which satisfy the above condition. For SE, the free parameters w, w_s and n are varied to match Λ . Clearly the same Λ value can occur for many combinations of $(c_b, \alpha_b), (c_p, \alpha_p), (c_e, \alpha_e)$, and (w, w_s, n) .

Our analysis of these combinations reveals the following: different ensembles indeed undergo almost similar evolutions qualitatively if the entropies are rescaled by their maximum value, referred here as $\langle R_1(\Lambda) \rangle_{max}$ for a fixed Λ . This is indeed indicated by the illustrations in Figs. 6 and 7, depicting L_A -dependence of $\frac{\langle R_1 \rangle}{\langle R_1 \rangle_{max}}$ and $\frac{\langle R_2 \rangle}{\langle R_2 \rangle_{max}}$ for six values of Λ ranging from $10 \rightarrow 10^6$. Here the bi-partition, i.e., the ‘‘cut’’ at which $\langle R_n \rangle$ is maximum, for a fixed Λ , can be derived from Eqn. (26) by invoking the condition $\frac{\partial \langle R_n \rangle}{\partial L_A} = 0$; the corresponding value of L_A is later referred as L_m . (We re-emphasize here the difference between $\langle R_n \rangle_{max}$ and $R_{n,\infty}$: while the former is the maximum entanglement entropy for a fixed Λ , the latter is the limit reached at $\Lambda \rightarrow \infty$, a maximum limit for the ensemble). But as Λ can depend on L_A explicitly as well as through ensemble parameters (non-trivially as indicated by our critical point analysis discussed above), in order to keep it fixed, its explicit variation with respect to L_A must be balanced by other system parameters, e.g., α in BE, PE and EE. we note that, in case of SE, balancing can occur due to different combinations of ensemble parameters.

As Figs. 6(a)-6(d) and 7(a)-7(d) indicate, the size-dependence of the entanglement entropy for small Λ values is non-trivial, first increasing and then decreasing. Based on our theoretical prediction Eqn. (26), this arises from a competition between the terms $g_n(\Lambda)$ and $L^{-\frac{\Lambda}{D_n}}$, former increasing and latter decreasing with L_A . Intuitively, a physical origin of small- Λ behaviour can be explained as follows. A small Λ corresponds to a state with lower participation ratio: the number of bases contributing significantly are restricted. As we change the subsystem size, L_A , the Hilbert space dimension increases exponentially, but the basis participation remains fixed and small. After a certain point, when $L_A = L_m$, the ‘‘effective’’ Hilbert space dimension becomes incommensurate to this exponential increase, leading to a fall in entropy. In fact, the Figs. 6(a)-6(c) and 7(a)-7(c) resembles the evolution of entanglement entropy (referred as Page-curve) in black hole physics [48]; a fermionic model proposed in this context, argues that the Page-curve behaviour amounts to

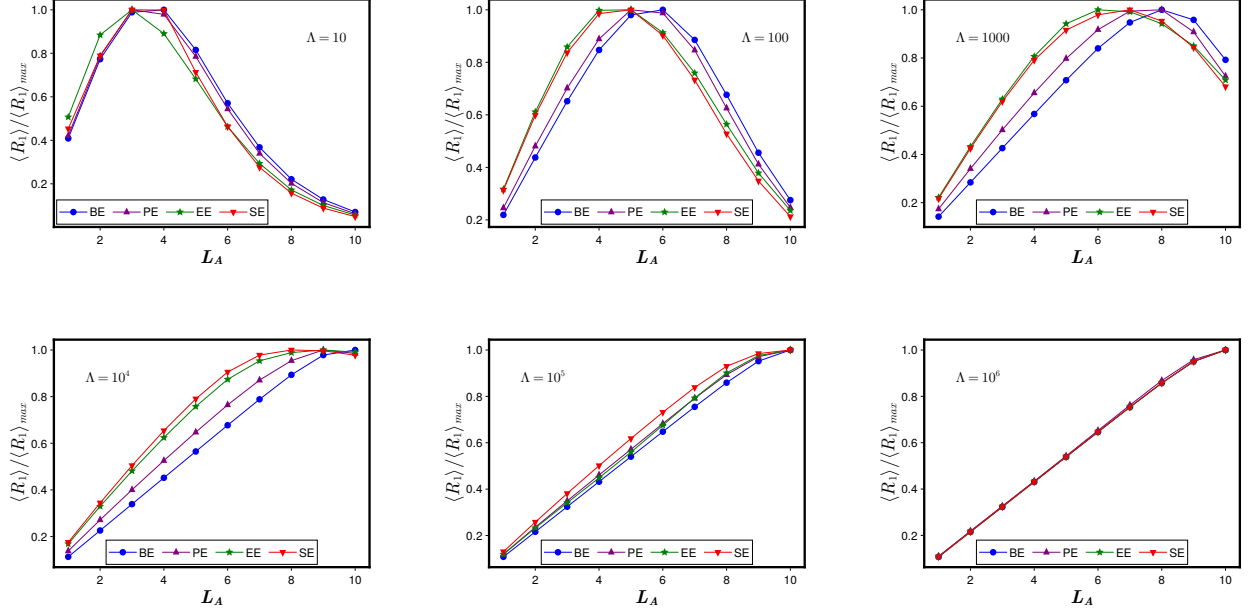


FIG. 6: The scaling of normalized R_1 with sub-system size L_A , ranging from $1 \rightarrow 10 (= \frac{L}{2})$, is shown for increasing ergodicity (increasing Λ) in the quantum state from (a) $\Lambda \sim 10$ to (f) $\Lambda \sim 10^6$. The qualitative similarity among the ensembles signifies the universality of Λ .

the effective Hilbert space dimension of the sub-system becoming small.

On the contrary, for a large but fixed Λ , the term $L^{-\frac{\Lambda}{D_n}}$ remains small. As a consequence, the pre-factor $g_n(\Lambda)$ dominates the growth, leading to $\langle R_n \rangle(\Lambda) \approx \langle R_n \rangle_{max}$. We also note that, for Λ fixed at large values, peak shifts to larger L_A range. Typically, the entropy of an ergodic state is believed to be the maximum when the partition is balanced, *i.e.*, at $L_A = \frac{L}{2}$ [14] and is expected to follow a volume-law scaling, *i.e.*, Eqn. (34) with $q_1 \neq 0, q_2 = 0$. This is indeed confirmed by the displays in Figs. 6(e), 6(f), 7(e), and 7(f) in the large Λ -regime.

It is worth re-emphasizing the roles of Λ_{ent} and Λ in characterizing the entanglement universality classes. As Eqn. (26) indicates, $\Lambda_{ent} = \frac{\Lambda}{D_n}$ is the single functional of the system parameters that governs the variation of entanglement entropy for any combination of system parameters including subsystem sizes. Different ensembles with same Λ_{ent} , even though the latter may arise from different combinations of system parameters, are predicted to have same entanglement entropy if they are subjected to same constants of evolution. More clearly, our theory predicts same entanglement entropy for two ensembles with same Λ_{ent} values even if they correspond to different subsystem sizes. This is however not the case

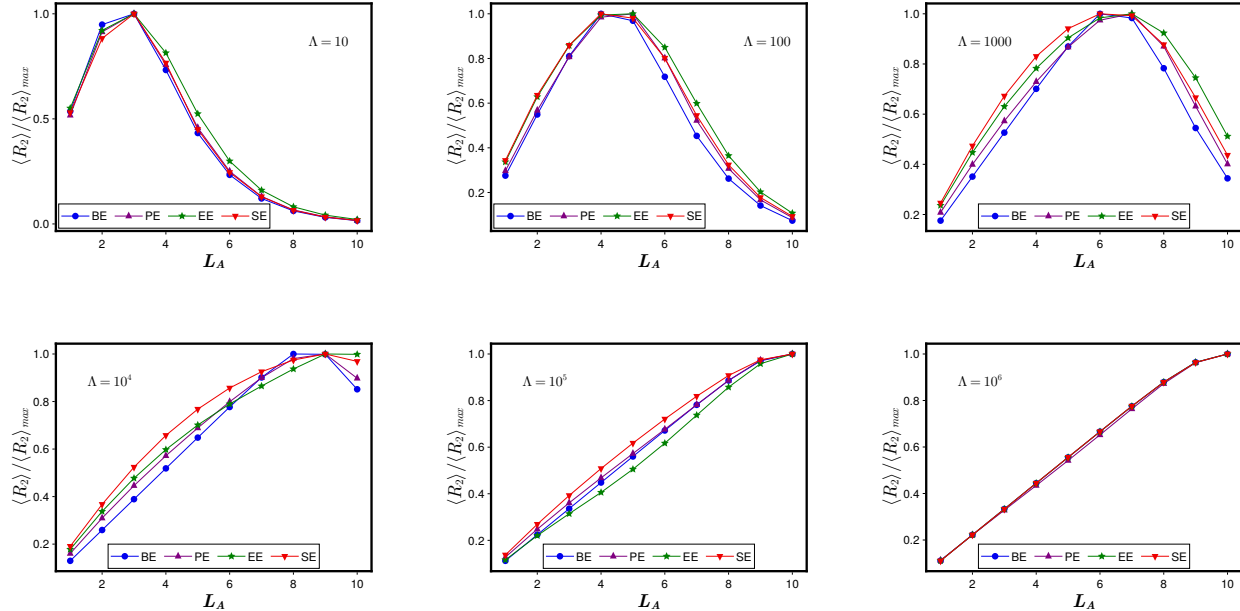


FIG. 7: The scaling of normalized R_2 with sub-system size L_A is shown for the same cases as for R_1 in Figs. 6.

if only their Λ values are same; now the analogy is only qualitative and occurs for the “ratio” of entanglement entropy and only if the ensembles have same subsystem sizes. Clearly Λ_{ent} characterizes more robust universality class of the entanglement entropy and Λ only the sub universality classes.

IV. CONCLUSION

In the end, we summarize our main results and insights and open questions. Growing potential relevance of multiparametric Gaussian states as an easy resource in quantum information motivated us in [15] to analyse their entanglement statistics. The study predicted that a broad range of non-ergodic bipartite pure states, within a same universality class of global constraints, can further be classified into sub-universality classes characterized by the complexity parameter Λ . But a detailed numerical analysis, described in present study, reveals that a robust form of universality, insensitive even to subsystem sizes, can be achieved only in terms of Λ_{ent} , obtained by a rescaling of Λ by another system-dependent parameter D_n . As Λ_{ent} can take continuous values between zero (initial state) and infinity (maximum

entanglement), this indicates, for finite system sizes, the existence of an infinite number of universality classes lying between separability and maximal entanglement limits.

Besides identification of the correct parameter Λ_{ent} leading to universality, another important contribution of the present work is to analyse the separate roles of two complexity scales, i.e., Λ and D_n . As discussed in main text, a knowledge of Λ is sufficient to predict the evolution of the entropy of a non-ergodic pure state represented by a multiparametric Gaussian ensemble (details of all ensemble parameters not required), but its rescaling by D_n is necessary for a comparison of the different states; D_n seems to have its origin in a "rescaling" of the Schmidt eigenvalues which enter in entanglement entropy. For deeper insights in the exact role of Λ , we have also analysed the variation of entropy with subsystem size while keeping Λ as well as full system size fixed; this in turn requires readjustment of other system parameters. For a large but fixed Λ , the state approaches ergodic, equivalently, maximum entanglement limit as the subsystem size increases and obeys the standard volume-law. For smaller Λ , the entropy first increases for small system sizes to a maximum and then decreases; this behaviour seems to be arising from a competition between two different tendencies of the quantum correlations, namely, the one pushing towards their homogeneity (indicated by increasing entanglement between two subsystems) and the noise, appearing through D_n , characterizing hindrance to homogeneity. We also find that the states with same Λ undergo qualitatively analogous evolution of the rescaled entanglement entropy as L_A varies; this reveals a hidden connection and a possible classification of the states based on complexity parameter Λ .

An important aspect of our analysis is the consideration of the state matrix ensembles represented by an ensemble density in a multiparametric Gaussian form: the latter extends applicability of our results to a broad range of non-ergodic states with independent Gaussian components. The appearance of such states in wide-ranging areas, from black holes to nanophysics, renders a rich potential applicability to our results.

The present study has focussed on non-ergodic pure Gaussian states with complex components in the bipartite basis. A straightforward extension of our analysis is possible for the states with real coefficients; such bipartite states can appear in case of many-body systems with time-reversal symmetry and integer angular momentum. A derivation of common mathematical formulation similar to the one discussed here as well as in [15] for mixed states or multipartite states is also very desirable. Further while our present analysis as well as

in [15] is confined to multiparametric Gaussian ensembles of state matrices, we intuitively believe the results will be applicable for non-Gaussian state matrices too. This needs to be verified.

V. ACKNOWLEDGEMENT

D.S. is supported by the MHRD under the PMRF scheme (ID 2402341) and P.S. is grateful to SERB, DST, India for the financial support provided for the research under Matrics grant scheme.

-
- [1] M. A. Nielsen and I. L. Chuang, *Quantum computation and quantum information*. Cambridge university press, 2010.
- [2] G. A. et al., “Countering a fundamental law of attraction with quantum wave-packet engineering,” *Annales Henri Poincare*, vol. 5, p. 013150, 2023.
- [3] C. W. et. al., “Gaussian quantum information,” *Review of Modern Physics*, vol. 84, no. 2, p. 621, 2012.
- [4] I. NECHITA, “Applications of random matrices in quantum information theory,” *Notes for ICMAT in Madrid*, 2019.
- [5] B. Collins and I. Nechita, “Random matrix techniques in quantum information theory,” *Journal of Mathematical Physics*, vol. 57, no. 1, 2016.
- [6] W. Brown and O. Fawzi, “Short random circuits define good quantum error correcting codes,” in *2013 IEEE International Symposium on Information Theory*, pp. 346–350, IEEE, 2013.
- [7] S. Choi, Y. Bao, X.-L. Qi, and E. Altman, “Quantum error correction in scrambling dynamics and measurement-induced phase transition,” *Physical Review Letters*, vol. 125, no. 3, p. 030505, 2020.
- [8] K. Zyczkowski and H.-J. Sommers, “Induced measures in the space of mixed quantum states,” *Journal of Physics A: Mathematical and General*, vol. 34, no. 35, p. 7111, 2001.
- [9] F. Haake, *Quantum signatures of chaos*. Springer, 1991.
- [10] E. Bogomolny and M. Sieber, “Eigenfunction distribution for the rosenzweig-porter model,” *Physical Review E*, vol. 98, no. 3, p. 032139, 2018.
- [11] L. Wei, “Average capacity of quantum entanglement,” *Journal of Physics A: Mathematical and Theoretical*, vol. 56, p. 015302, 2022.
- [12] E. Bianchi, L. Hackl, and M. Kieburg, “Page curve for fermionic gaussian states,” *Physical Review B*, vol. 103, no. 24, p. L241118, 2021.
- [13] Y. Huang and L. Wei, “Entropy fluctuation formulas of fermionic gaussian states,” *Annales Henri Poincare*, vol. 24, no. 2, p. 4283, 2023.
- [14] D. N. Page, “Average entropy of a subsystem,” *Physical review letters*, vol. 71, no. 9, p. 1291, 1993.

- [15] D. Shekhar and P. Shukla, “Entanglement dynamics of multi-parametric random states: a single parametric formulation,” *Journal of Physics A: Mathematical and Theoretical*, vol. 56, p. 265303, jun 2023.
- [16] R. Horodecki, P. Horodecki, M. Horodecki, and K. Horodecki, “Quantum entanglement,” *Reviews of modern physics*, vol. 81, no. 2, p. 865, 2009.
- [17] G. Vidal, J. I. Latorre, E. Rico, and A. Kitaev, “Entanglement in quantum critical phenomena,” *Phys. Rev. Lett.*, vol. 90, p. 227902, Jun 2003.
- [18] A. Kitaev and J. Preskill, “Topological entanglement entropy,” *Phys. Rev. Lett.*, vol. 96, p. 110404, Mar 2006.
- [19] R. Nandkishore and D. A. Huse, “Many-body localization and thermalization in quantum statistical mechanics,” *Annual Review of Condensed Matter Physics*, vol. 6, pp. 15–38, 3 2015.
- [20] D. J. Luitz, N. Laflorencie, and F. Alet, “Many-body localization edge in the random-field heisenberg chain,” *Physical Review B*, vol. 91, p. 081103, 2 2015.
- [21] Q. Zhang and G.-M. Zhang, “Noise-induced entanglement transition in one-dimensional random quantum circuits,” *Chinese Physics Letters*, vol. 39, no. 5, p. 050302, 2022.
- [22] B. Skinner, J. Ruhman, and A. Nahum, “Measurement-induced phase transitions in the dynamics of entanglement,” *Physical Review X*, vol. 9, p. 031009, 7 2019.
- [23] X.-L. Qi, “Does gravity come from quantum information?,” *Nature Physics*, vol. 14, pp. 984–987, 10 2018.
- [24] M. L. Mehta, *Random matrices*. Elsevier, 2004.
- [25] M. V. Berry, “Regular and irregular semiclassical wavefunctions,” *Journal of Physics A: Mathematical and General*, vol. 10, no. 12, p. 2083, 1977.
- [26] The conjecture states that the eigenfunctions of a classically ergodic system ought to evince Gaussian random behaviour, as though they were random waves, in the large eigenvalue limit.
- [27] P. Shukla, “Eigenfunction statistics of wishart brownian ensembles,” *Journal of Physics A: Mathematical and Theoretical*, vol. 50, p. 435003, oct 2017.
- [28] A. Gleit and A. J. Lazar, “Basis constants for the space of $n \times n$ matrices,” *Journal of Functional Analysis*, vol. 22, no. 4, pp. 354–365, 1976.
- [29] L. Vidmar, L. Hackl, E. Bianchi, and M. Rigol, “Volume law and quantum criticality in the entanglement entropy of excited eigenstates of the quantum ising model,” *Physical review*

- letters*, vol. 121, no. 22, p. 220602, 2018.
- [30] K. Audenaert, J. Eisert, M. B. Plenio, and R. F. Werner, “Entanglement properties of the harmonic chain,” *Physical Review A*, vol. 66, no. 4, p. 042327, 2002.
- [31] A. Osterloh, L. Amico, G. Falci, and R. Fazio, “Scaling of entanglement close to a quantum phase transition,” *Nature*, vol. 416, no. 6881, pp. 608–610, 2002.
- [32] T. J. Osborne and M. A. Nielsen, “Entanglement in a simple quantum phase transition,” *Phys. Rev. A*, vol. 66, p. 032110, Sep 2002.
- [33] L. Ding, N. Bray-Ali, R. Yu, and S. Haas, “Subarea law of entanglement in nodal fermionic systems,” *Physical review letters*, vol. 100, no. 21, p. 215701, 2008.
- [34] M. M. Wolf, “Violation of the entropic area law for fermions,” *Physical review letters*, vol. 96, no. 1, p. 010404, 2006.
- [35] D. Gioev and I. Klich, “Entanglement entropy of fermions in any dimension and the widom conjecture,” *Physical review letters*, vol. 96, no. 10, p. 100503, 2006.
- [36] W. Li, L. Ding, R. Yu, T. Roscilde, and S. Haas, “Scaling behavior of entanglement in two- and three-dimensional free-fermion systems,” *Physical Review B*, vol. 74, no. 7, p. 073103, 2006.
- [37] M. Cramer, J. Eisert, and M. Plenio, “Statistics dependence of the entanglement entropy,” *Physical review letters*, vol. 98, no. 22, p. 220603, 2007.
- [38] M. B. Hastings, “An area law for one-dimensional quantum systems,” *Journal of statistical mechanics: theory and experiment*, vol. 2007, no. 08, p. P08024, 2007.
- [39] P. Calabrese and J. Cardy, “Entanglement entropy and quantum field theory,” *Journal of statistical mechanics: theory and experiment*, vol. 2004, no. 06, p. P06002, 2004.
- [40] E. Fradkin and J. E. Moore, “Entanglement entropy of 2d conformal quantum critical points: hearing the shape of a quantum drum,” *Physical review letters*, vol. 97, no. 5, p. 050404, 2006.
- [41] A. B. Kallin, M. B. Hastings, R. G. Melko, and R. R. Singh, “Anomalies in the entanglement properties of the square-lattice heisenberg model,” *Physical Review B*, vol. 84, no. 16, p. 165134, 2011.
- [42] M. A. Metlitski and T. Grover, “Entanglement entropy of systems with spontaneously broken continuous symmetry,” *arXiv preprint arXiv:1112.5166*, 2011.
- [43] M. Levin and X.-G. Wen, “Detecting topological order in a ground state wave function,” *Phys. Rev. Lett.*, vol. 96, p. 110405, Mar 2006.

- [44] M. Haque, O. Zozulya, and K. Schoutens, “Entanglement entropy in fermionic Laughlin states,” *Physical Review Letters*, vol. 98, no. 6, p. 060401, 2007.
- [45] J. Preskill, “Lecture notes for physics 229: Quantum information and computation,” *California Institute of Technology*, vol. 16, no. 1, pp. 1–8, 1998.
- [46] E. Bianchi, L. Hackl, M. Kieburg, M. Rigol, and L. Vidmar, “Volume-law entanglement entropy of typical pure quantum states,” *PRX Quantum*, vol. 3, no. 3, p. 030201, 2022.
- [47] J. Eisert, M. Cramer, and M. B. Plenio, “Colloquium: Area laws for the entanglement entropy,” *Reviews of Modern Physics*, vol. 82, no. 1, p. 277, 2010.
- [48] S. Kehrein, “Page curve entanglement dynamics in an analytically solvable model,” *arXiv preprint arXiv:2311.18045*, 2023.

Appendix A: Derivation of Eqn.(14)

The ensemble average for any arbitrary function $F(\lambda_1, \dots, \lambda_N)$ can be defined as

$$\langle F(\Lambda, S_1) \rangle = C_{hs} \int F_n(r) \delta \left(S_1 - \sum_k \lambda_k \right) P_\lambda D\lambda \quad (\text{A1})$$

where J gives the normalization condition for the *jpdf* of the Schmidt eigenvalues under trace constraint $S_1 = \sum \lambda_k$:

$$J = C_{hs} \int \delta \left(S_1 - \sum_k \lambda_k \right) P_\lambda D\lambda \quad (\text{A2})$$

Choosing $J = 1$ subjects P_λ to following normalization condition: $\int \delta (S_1 - \sum_k \lambda_k) P_\lambda D\lambda = C_{hs}^{-1}$.

As discussed in detail in [15], for any arbitrary function $F(\lambda_1, \dots, \lambda_N)$ we have (choosing $J = 1$)

$$\begin{aligned} \frac{\partial \langle F \rangle}{\partial Y} &= \alpha \langle F \rangle + \frac{\partial}{\partial S_1} \left(2 \gamma S_1 - \frac{1}{2} \beta N(N + 2\nu - 1) \right) \langle F \rangle + \beta \left\langle \sum_{m,n=1}^N \frac{\partial F}{\partial \lambda_n} \frac{\lambda_n}{\lambda_n - \lambda_m} \right\rangle \\ &- \left\langle \sum_{n=1}^N \frac{\partial F}{\partial \lambda_n} (-\beta\nu + 2\gamma\lambda_n) \right\rangle + \left\langle \sum_{n=1}^N \frac{\partial^2 F}{\partial \lambda_n^2} \lambda_n \right\rangle - 2 \frac{\partial}{\partial S_1} \left\langle \sum_{n=1}^N \frac{\partial F}{\partial \lambda_n} \lambda_n \right\rangle + \frac{\partial^2}{\partial S_1^2} (S_1 \langle F \rangle) \end{aligned} \quad (\text{A3})$$

where $\alpha = \frac{\partial \log C_{hs}}{\partial Y}$ with C_{hs} as a normalization constant for the JPDPF P_c [15]: $\int P_c(\Lambda) D\Lambda = C_{hs} J$. As $\log C_{hs}$ varies slowly with Y , we have $\frac{\alpha}{NN_\nu} \approx 0$ and the contribution from corresponding term can be ignored for simplification.

Solution for R_1 : Using $F = R_1$ where $R_1 = -\sum_n \lambda_n \log \lambda_n$ in eq.(A3), we have (details discussed in [15])

$$\begin{aligned} \frac{1}{NN_\nu} \frac{\partial \langle R_1(S_1) \rangle}{\partial Y} &= \frac{\beta}{2N} \langle R_0 \rangle - \frac{1}{2} \left[\beta + \frac{\beta(N-1)}{N_\nu} - \frac{4S_1}{NN_\nu} + \frac{2(N-2)}{NN_\nu} \right] + \\ &- \frac{1}{2} \left(\beta N - \frac{4S_1}{NN_\nu} \right) \frac{\partial \langle R_1 \rangle}{\partial S_1} + \frac{S_1}{NN_\nu} \frac{\partial^2 \langle R_1 \rangle}{\partial S_1^2} \end{aligned} \quad (\text{A4})$$

with $N_\nu = N + 2\nu - 1$, and $R_0 = -\sum_n \log \lambda_n$. As our interest is in $S_1 = 1$ condition only, we consider the variation of S_1 only in the neighbourhood of $S_1 \sim 1$.

For trace condition $S_1 = \sum_k \lambda_k$ on N eigenvalues λ_k , we have $S_1/N \leq \lambda_k \leq S_1$, thereby implying $-S_1 \log S_1 \leq R_1 \leq \log N - S_1 \log S_1$ and $N \log(\frac{N}{S_1}) \leq R_0 \leq \infty$. Thus, for $S_1 \sim 1$, the contribution from the terms with partial derivatives i.e., $\frac{S_1}{N^2} \frac{\partial^2 \langle R_1 \rangle}{\partial S_1^2}$ and $\frac{2}{N^2} \frac{\partial J}{\partial S_1}$ can be neglected as compared to other terms in eq.(A4). Further as α corresponds to a logarithmic response of the normalization factor C_{hs} to a change in Y , this is also expected to be negligible in units of NN_ν . The resulting differential equation using the rescaled parameter $\Lambda = N N_\nu (Y - Y_0)$ becomes

$$\frac{2}{\beta} \frac{\partial \langle R_1 \rangle}{\partial \Lambda} = g_1(\Lambda, S_1) - \frac{\partial \langle R_1 \rangle}{\partial S_1}, \quad (\text{A5})$$

with $g_1(\Lambda, S_1) = \left(\frac{\langle R_0 \rangle}{N} - q_0 \right)$ with $q_0 = \frac{N_\nu + (N-1)}{N_\nu}$.

The above equation can be solved by using the standard method of characteristics for partial differential equations. The characteristic equations are

$$\frac{d\Lambda}{2/\beta} = \frac{dS_1}{1} = \frac{d\langle R_1 \rangle}{g_1} \quad (\text{A6})$$

The general solution of eq.(A6) is given by the function $F_1(\Phi, \Psi) = 0$ or equivalently $\Phi = f(\Psi)$ where F_1, f are arbitrary functions and the functions $\Phi(\langle R_1 \rangle, \Lambda, S_1)$ and $\Psi(\langle R_1 \rangle, \Lambda, S_1)$ are obtained by solving any of the two pairs of eq.(A6). We have, from first pair,

$$d\Phi \equiv d \left(S_1 - \frac{\beta\Lambda}{2} \right) = 0 \quad (\text{A7})$$

The above gives

$$\Phi = \left(S_1 - \frac{\beta\Lambda}{2} \right) \quad (\text{A8})$$

From second pair, we have,

$$d\langle R_1 \rangle - g_1 dS_1 = 0 \quad (\text{A9})$$

The above in turn gives

$$\Psi = \langle R_1 \rangle - \int g_1 dS_1 \quad (\text{A10})$$

The general solution of eq.(A6) can now be given as $F(\Psi, \Phi) = 0$ with F as an arbitrary function. Equivalently we can write $\Psi = f(\Phi)$ with $f(S_1, \Lambda) \equiv f \left(S_1 - \frac{\beta\Lambda}{2} \right)$ as an arbitrary function and $I_1 \equiv \int g_1 dS_1$. This in turn gives

$$\langle R_1 \rangle(\Lambda, S_1) = I_1 + f \left(S_1 - \frac{\beta\Lambda}{2} \right) \quad (\text{A11})$$

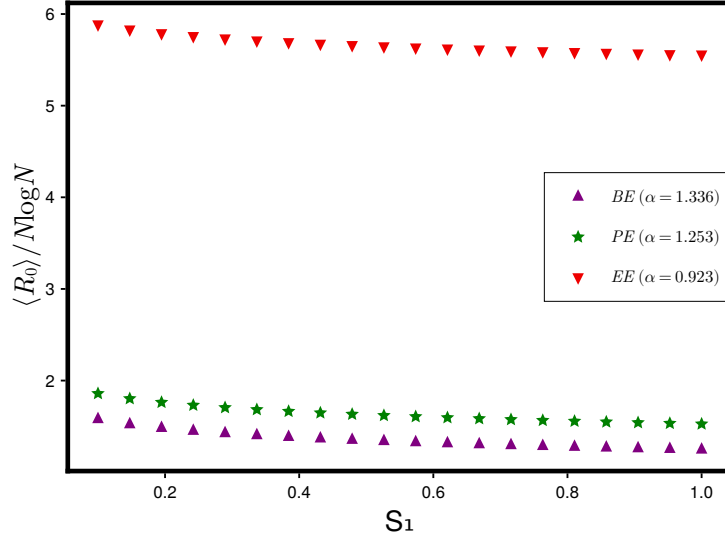


FIG. 8: $\langle R_0 \rangle$ -dependence on S_1 : The figure displays the evolution of $\langle R_0 \rangle$ with S_1 for BE, PE and EE. As can be seen from the figure, R_0 is almost constant near $S_1 \sim 1$.

The integral I_1 over S_1 can further be approximated by noting that $\langle R_0 \rangle$ changes very slowly with S_1 i.e., $R_0 \sim -\log S_1$. (This can be seen by writing $R_0 = -\sum_{n=1}^N \log \lambda_n$ in terms of constraint $S_1 = \sum_{n=1}^N \lambda_n$. This leads to $R_0 = -\sum_{n=1}^{N-1} \log \lambda_n - \log \left(S_1 - \sum_{n=1}^{N-1} \lambda_n \right) = -\log S_1 - \sum_{n=1}^{N-1} \left(\frac{\lambda_n}{S_1} + \log \lambda_n \right)$. This is also supported by figure(8) displaying the $\langle R_0 \rangle$ -dependence on S_1 for BE, PE and EE). The above permits the approximation $\int g_1 dS_1 \approx g_1 S_1$. and leads to, for $S_1 = 1$,

$$\langle R_1 \rangle(\Lambda, 1) = g_1(\Lambda, 1) + f \left(1 - \frac{\beta \Lambda}{2} \right) \quad (\text{A12})$$

As $\langle R_1(0, 1) \rangle = 0$ for a separable initial state chosen at $Y = Y_0$ i.e., $\Lambda = 0$, we have $f(0, 1) = -g_1(0, 1)$. Further to satisfy the boundary condition at $\Lambda \rightarrow \infty$, we must have $f(\infty, 1) = \langle R_1(\infty, 1) \rangle - g_1(\infty, 1)$. But as $g_1(\infty, 1) \approx \frac{\langle R_0(\infty, 1) \rangle}{N} \approx \langle R_1(\infty, 1) \rangle$, this implies $f(\infty, 1) \approx 0$. One possible form of f that satisfies the above conditions on f can be given as $f(\Lambda, 1) = -g_1(\Lambda, 1) L^{-\tau(1-(\beta\Lambda/2))}$; the latter leads to $\langle R_1 \rangle(\Lambda, 1) = g_1(\Lambda, 1) (1 - L^{-\tau(1-(\beta\Lambda/2))})$.

Solution for R_2 : Similarly using $F = R_2$ where $R_2 = -\log \sum_{k=1}^N \lambda_k^2$ in eq.(A3), we have

$$\begin{aligned} \frac{\partial \langle R_2(S_1) \rangle}{\partial Y} &= 2\gamma \langle R_2 \rangle - (2\beta(N + \nu - 1) + 2) S_1 \left\langle \frac{1}{S_2} \right\rangle + 4 \left\langle \frac{S_3}{S_2^2} \right\rangle + 4 + \\ &+ S_1 \frac{\partial^2 \langle R_2 \rangle}{\partial S_1^2} + (2S_1 - \frac{1}{2}\beta N(N + 2\nu - 1) + 2) \frac{\partial \langle R_2 \rangle}{\partial S_1} \end{aligned} \quad (\text{A13})$$

Using similar approximations as in R_1 case, the resulting differential equation using the rescaled parameter $\Lambda = N N_\nu (Y - Y_0)$ now becomes

$$\frac{2}{\beta} \frac{\partial \langle R_2 \rangle}{\partial \Lambda} = g_2(\Lambda, S_1) - \frac{\partial \langle R_2 \rangle}{\partial S_1}, \quad (\text{A14})$$

with $g_2(\Lambda, S_1) = -\eta S_1 \left\langle \frac{1}{S_2} \right\rangle$ (with $\frac{1}{S_1^2} \leq \frac{1}{S_2} \leq \frac{N}{S_1^2}$), where, $\eta = \frac{2\beta(N+\nu-1)}{N(N+2\nu-1)}$. Proceeding as in previous case, the solution of the above equation can be given as

$$\langle R_2 \rangle(\Lambda, S_1) = I_2(\Lambda, S_1) + f \left(S_1 - \frac{\beta \Lambda}{2} \right) \quad (\text{A15})$$

Proceeding as in the case of I_1 , here again $I_2 = \int g_2 dS_1$ can be approximated by noting that $\left\langle \frac{1}{S_2} \right\rangle$ changes very slowly near $S_1 = 1$; this in turn permits $I_2 \approx -\frac{\eta}{2} \left\langle \frac{1}{S_2} \right\rangle S_1^2$ and leads to, for $S_1 = 1$,

$$\langle R_2 \rangle(\Lambda, 1) = \frac{1}{2} g_2(\Lambda, 1) + f \left(1 - \frac{\beta \Lambda}{2} \right) \quad (\text{A16})$$

The form of function f in the above can be fixed by invoking boundary conditions: with $\langle R_2(0, 1) \rangle = 0$ for a separable initial state chosen at $Y = Y_0$ i.e., $\Lambda = 0$, f must satisfy the condition that $f(0, 1) = -\frac{1}{2} g_2(0, 1)$. Similarly with $\langle R_2(\infty, 1) \rangle = -\frac{1}{2} g_2(\infty, 1)$, we have $f(\infty, 1) = \langle R_2(\infty, 1) \rangle - \frac{1}{2} g_2(\infty, 1) = -g_2(\infty, 1)$. The above conditions on f can again be satisfied for $f(\Lambda, 1) = -g_2(\Lambda, 1) + \frac{1}{2} g_2(\Lambda, 1) L^{-\tau(1-(\beta \Lambda/2))}$ with τ as an arbitrary constant. For $S_1 = 1$, the above leads to $\langle R_2 \rangle(\Lambda, 1) = -\frac{1}{2} g_2(\Lambda, 1) (1 - L^{-\tau(1-(\beta \Lambda/2))})$.

Appendix B: Solution for R_0

Using $F = R_0$ where $R_0 = -\sum_{k=1}^N \log \lambda_k$ in eq.(A3), we have

$$\begin{aligned} \frac{\partial \langle R_0(S_1) \rangle}{\partial Y} &= 2\gamma \langle R_0 \rangle + (2S_1 - \frac{1}{2}\beta N(N+2\nu-1)) \frac{\partial \langle R_0 \rangle}{\partial S_1} + (1-\beta\nu) \langle S_{-1} \rangle \\ &+ 2N + \frac{\partial^2 S_1 \langle R_0 \rangle}{\partial S_1^2} \end{aligned} \quad (\text{B1})$$

where $\nu = \frac{(N_B - N_A + 1)}{2}$. Further S_m is defined as (with m as a positive/ negative integer)

$$S_m \equiv \sum_{k=1}^N \lambda_k^m. \quad (\text{B2})$$

Here $\langle S_{-1} \rangle$ ranges from $N^2/S_1 \leq S_{-1} \leq \infty$. We also note that $S_{-1} \gg R_0$ and therefore the former can be treated as almost constant while $\langle R_0 \rangle$ varies with Λ .

For simplification here we consider the balanced case $N_A = N_B$ and the case $\beta = 2$. This gets rid of the term S_{-1} . Proceeding again as in R_1 -case, the above equation can be approximated as

$$\frac{\partial \langle R_0(S_1) \rangle}{\partial \Lambda} = \frac{2\gamma \langle R_0 \rangle}{N^2} + \frac{2}{N} - \frac{\partial \langle R_0 \rangle}{\partial S_1}. \quad (\text{B3})$$

Further solving the equation as in R_1 case above, we have, for arbitrary S_1 ,

$$\log \left(\frac{2\gamma \langle R_0 \rangle}{N^2} + \frac{2}{N} - \phi_0 \right) = \frac{2\gamma}{N^2} S_1 + f_0(\Lambda - S_1) \quad (\text{B4})$$

with $f_0(\Lambda, S_1) \equiv f_0(\Lambda - S_1)$ as an arbitrary function and ϕ_0 a constant of integration. Inverting the above gives

$$\langle R_0 \rangle(\Lambda, S_1) = \frac{N^2}{2\gamma} e^{f_0(\Lambda - S_1) + \frac{2\gamma S_1}{N^2}} - \frac{2N}{2\gamma} + \phi_0 \quad (\text{B5})$$

The unknown constant ϕ_0 can now be determined by invoking the boundary condition at $\Lambda \rightarrow \infty$. Eq.(B5) gives $\phi_0 = \langle R_0 \rangle(\infty, S_1) - \frac{N^2}{2\gamma} e^{f_0(\infty - S_1) + \frac{2\gamma S_1}{N^2}} + N$. This in turn gives

$$\langle R_0 \rangle(\Lambda, S_1) = \langle R_0 \rangle(\infty, S_1) + \frac{N^2}{2\gamma} e^{\frac{2\gamma S_1}{N^2}} (e^{f_0(\Lambda - S_1)} - e^{f_0(\infty - S_1)}) \quad (\text{B6})$$

The form of f_0 can now be determined by substituting eq.(B5) in eq.(B3). This leads to

$$\frac{\partial f_0}{\partial \Lambda} = -\frac{\partial f_0}{\partial S_1}. \quad (\text{B7})$$

A particular solution of the above, satisfying required boundary conditions at $\Lambda = 0, \infty$, can be given as $f_0 = -\log(\Lambda - S_1)\tau$ with τ as an unknown constant. This on substitution in eq.(B6) along with $S_1 = 1$ gives

$$\begin{aligned} \langle R_0 \rangle(\Lambda, 1) &= \langle R_0 \rangle(\infty, 1) + \frac{N^2}{2\gamma(\Lambda - 1)\tau} \exp \left[\frac{2\gamma}{N^2} \right] \\ &\approx \langle R_0 \rangle(\infty, 1) + \frac{N^2}{2\gamma(\Lambda - 1)\tau} \end{aligned} \quad (\text{B8})$$

where the 2nd equality is obtained by the approximation $e^{2\gamma/N^2} \approx 1 + \frac{2\gamma}{N^2}$

Appendix C: Solution for $\langle \frac{1}{S_2} \rangle$

Using $F = \frac{1}{S_2}$ where $S_2 = \sum_{k=1}^N \lambda_n^2$ in eq.(A3) and proceeding as in previous cases, the dependence of $\frac{1}{S_2}$ can be derived. Using notation $Q \equiv \frac{1}{S_2}$, we have

$$\begin{aligned} \frac{\partial \langle Q \rangle}{\partial Y} &= 6\gamma \langle Q \rangle + (4 + 2S_1 - \frac{1}{2}\beta N(N + 2\nu - 1)) \frac{\partial \langle Q \rangle}{\partial S_1} - (2\beta(N - 1) + 2\beta\nu + 2)S_1 \langle Q^2 \rangle \\ &+ 8 \langle S_3 Q^3 \rangle + \frac{\partial^2 S_1 \langle Q \rangle}{\partial S_1^2} \end{aligned} \quad (C1)$$

with all symbols same meaning as in previous appendix.

For simplification here we consider the balanced case $N_A = N_B$. Further noting that typically $\frac{1}{N^k} \leq S_{k+1} \leq 1$ and $1 \leq Q \leq N$, the terms with $\langle S_3 Q^3 \rangle$ and $6\gamma \langle Q \rangle$ can be neglected with respect to $\langle Q^2 \rangle$. The above equation can then be approximated as

$$\frac{\partial \langle Q \rangle}{\partial \Lambda} \approx g_q - \frac{\partial \langle Q \rangle}{\partial S_1}. \quad (C2)$$

with $g_q \equiv \frac{2S_1\beta}{N} \langle Q^2 \rangle$.

Further solving the equation as in R_1 case above, we have, for arbitrary S_1 ,

$$\langle Q \rangle (\Lambda, S_1) = I_q(\Lambda, S_1) + f_q(\Lambda, S_1) \quad (C3)$$

where $I_q(\Lambda, S_1) \equiv \int g_q dS_1$ with $f_q(\Lambda, S_1) \equiv f_q(\Lambda - S_1)$ as an arbitrary function.

As $\langle Q(0, 1) \rangle = 1$ for a separable initial state at $\Lambda = 0$, we have $f_q(0, 1) = 1 - I_q(0, 1)$. Further as $\langle Q(\infty, 1) \rangle$ i.e., we must have $f_q(\infty, 1) = \langle Q(\infty, 1) \rangle - I_q(\infty, 1)$. The form of f_q that satisfies the above conditions can be given as $f(\Lambda, 1) = (\langle Q(\Lambda, 1) \rangle - I_q(\Lambda, 1)) e^{\tau(1-(\beta\Lambda/2))}$; the latter leads to

$$\langle Q \rangle (\Lambda, 1) = e^{\tau(1-(\beta\Lambda/2))} + I_q(\Lambda, 1) (1 - e^{\tau(1-(\beta\Lambda/2))}) \quad (C4)$$

with τ as an arbitrary function independent of Λ , subjected to conditions that in large N limit, $\tau \rightarrow 0$ but $\Lambda \geq \frac{1}{\tau}$. Here again, with Q^2 varying very slowly near $S_1 = 1$, $I_q(\Lambda, S_1)$ near $S_1 = 1$ can be approximated as $I_q(\Lambda, 1) = g_q(\Lambda, 1)/2 = \frac{\beta}{2N} \langle Q^2 \rangle$.

Appendix D: Λ_{ent} dependence of $R_{1,2}$

$$\langle \mathcal{R}_n \rangle = \mathcal{C}_{hs} \int \mathcal{R}_n(r) \delta \left(\mathcal{S}_1 - \sum_k r_k \right) P_r Dr \quad (\text{D1})$$

Differentiating the above equation with respect to Y_1 , substitution of eq.(17) in the right side of the above equation and proceeding as in [15], we have

$$\frac{1}{u_n} \frac{\partial \langle \mathcal{R}_n \rangle}{\partial \Lambda} = \tilde{g}_n(\Lambda, \mathcal{S}_1) - \frac{1}{v_n} \frac{\partial \langle \mathcal{R}_1 \rangle}{\partial \mathcal{S}_1}, \quad (\text{D2})$$

where $\tilde{g}_1(\Lambda, \mathcal{S}_1) = \frac{\langle \mathcal{R}_0 \rangle}{N}$, $\tilde{g}_2(\Lambda, \mathcal{S}_1) = -\frac{4\mathcal{S}_1}{N} \langle \frac{1}{S_2} \rangle$, $\tilde{g}_0(\Lambda, \mathcal{S}_1) = \frac{2\gamma}{N^2} (\langle \mathcal{R}_0 \rangle - N D)$ and $v_1 = 1$, $v_2 = \frac{\chi_2}{\chi_1}$, $v_0 \approx \frac{2D}{\beta}$ and $u_n = \frac{\chi_n \beta}{2D}$, $u_0 = 1$, $\chi_1 = \frac{N+2\nu D-1}{N+2\nu-1}$, $\chi_2 = \frac{N+\nu D-1}{N+2\nu-1}$.

Solutions for $\langle \mathcal{R}_1 \rangle$ and $\langle \mathcal{R}_2 \rangle$: Proceeding as in previous *appendices*, the general solution of eq.(D2) for $n = 1, 2$ can be given as

$$\langle \mathcal{R}_n \rangle(\Lambda, \mathcal{S}_1) = f(v_n \mathcal{S}_1 - u_n \Lambda) + v_n \mathcal{I}_n \quad n = 1, 2 \quad (\text{D3})$$

where $\mathcal{I}_n(\Lambda, \mathcal{S}_1) \equiv \int \tilde{g}_n d\mathcal{S}_1$.

Further using the rescaled constraint $\mathcal{S}_1 = \sum_n r_n = \frac{1}{D}$, we have

$$\langle \mathcal{R}_n \rangle \left(\Lambda, \frac{1}{D} \right) = f \left(\frac{v_n}{D} - u_n \Lambda \right) + v_n \mathcal{I}_n \quad (\text{D4})$$

Following from the relations in eqs.(20, 21), and using the boundary conditions on $\langle R_n \rangle$ i.e $\langle R_n \rangle(0, 1) = 0$ and $\langle R_n \rangle(\infty, 1) = L_A$, the boundary conditions for $\langle \mathcal{R}_n \rangle$ can be given as $\langle \mathcal{R}_n \rangle \left(0, \frac{1}{D} \right) = \frac{n \log D}{D}$ and $\langle \mathcal{R}_n \rangle \left(\infty, \frac{1}{D} \right) = \frac{L_A}{D} + \frac{n \log D}{D}$. These on substitution in eq.(D4) give the boundary condition on f : $\lim_{\Lambda \rightarrow 0} f \left(\frac{v_n}{D} - u_n \Lambda \right) = \frac{n \log D}{D} - v_n \mathcal{I}_n \left(0, \frac{1}{D} \right)$ and $\lim_{\Lambda \rightarrow \infty} f \left(\frac{v_n}{D} - u_n \Lambda \right) = \frac{n \log D}{D} + \frac{L_A}{D} - v_n \mathcal{I}_n \left(\infty, \frac{1}{D} \right)$.

Further, following from the relations in eqs.(20, 21), we have $\mathcal{I}_1(\Lambda, \mathcal{S}_1) \equiv \int \frac{\mathcal{R}_0}{N} d\mathcal{S}_1 = \frac{1}{D} \int \left(\frac{R_0}{N} + \log D \right) dS_1$. For $S_1 = 1$, this can again be approximated as (as in *appendix A*) $\mathcal{I}_1(\Lambda, \mathcal{S}_1) \approx \frac{1}{D} \left(\frac{R_0}{N} + \log D \right) = \frac{\mathcal{R}_0}{ND}$. Proceeding similarly, it can be shown that $\mathcal{I}_2(\Lambda, \frac{1}{D}) \approx -\frac{\eta}{2} \langle Q \rangle = I_2$.

The particular solution for f satisfying boundary conditions can now be given as $f \left(\frac{v_n}{D} - u_n \Lambda \right) = \frac{n \log D}{D} - v_n \mathcal{I}_n L_A^{\frac{(2v_n - \chi_n \beta \Lambda)}{2D}}$ (neglecting L_A/D in large N limit) . This in turn leads to

$$\langle \mathcal{R}_n \rangle \left(\Lambda, \frac{1}{D} \right) = v_n \mathcal{I}_n \left(1 - L_A \frac{(2v_n - \chi_n \beta \Lambda)}{2D} \right) + \frac{n \log D}{D} \quad (\text{D5})$$

with $\mathcal{I}_1 \approx \frac{\langle \mathcal{R}_0 \rangle}{ND}$ and $\mathcal{I}_2 \approx -\frac{\eta}{2} \frac{\langle \mathcal{Q} \rangle}{D^2}$.

Solution for $\langle \mathcal{R}_0 \rangle$: For $n = 0$ case of eq.(D2), the boundary conditions are different from those for $n = 1, 2$ and we need to proceed as in case of eq.(B3). The solution of eq.(D2) for $n = 0$ can be given as

$$\langle \mathcal{R}_0 \rangle \left(\Lambda, \frac{1}{D} \right) = \langle \mathcal{R}_0 \rangle(\infty, 1) + \frac{N^2 D}{2\gamma \Lambda} e^{\frac{2\gamma}{N^2}} + \frac{N \log D}{D} \quad (\text{D6})$$

Solution for $\langle \mathcal{Q} \rangle$: Using $\mathcal{Q}(r) = (\sum_k r_k^2)^{-1}$ and proceeding as before, we have

$$\langle \mathcal{Q} \rangle(\Lambda, \mathcal{S}_1) = \mathcal{C}_{hs} \int \left(\frac{1}{\sum_k r_k^2} \right) \delta \left(\mathcal{S}_1 - \sum_k r_k \right) P_r Dr. \quad (\text{D7})$$

Differentiation of the above equation with respect to Y_1 , using eq.(17) and proceeding as in *appendix C*, we have

$$\frac{\partial \langle \mathcal{Q} \rangle}{\partial Y_1} = \tilde{g}_s(\Lambda, \mathcal{S}_1) - v_s \frac{\partial \langle \mathcal{Q} \rangle}{\partial \mathcal{S}_1}, \quad (\text{D8})$$

where $\tilde{g}_s(\Lambda, \mathcal{S}_1) = -2\gamma \langle \mathcal{Q} \rangle + \frac{2\beta(N-1)\mathcal{S}_1 \langle \mathcal{Q}^2 \rangle}{D}$ and $v_s = \frac{\beta N^2}{2} - 2\gamma \mathcal{S}_1$. Proceeding as in *appendix C*, the general solution of eq.(D8) can be given as

$$\langle \mathcal{Q} \rangle(\Lambda, 1) = e^{\frac{\tau(1-\beta\Lambda)}{2}} + g_q(\Lambda, 1) \left(1 - e^{\frac{\tau(1-\beta\Lambda)}{2}} \right) \quad (\text{D9})$$

Appendix E: Complexity parameter formulation

A perturbation of the state by a change of the parameters $h_{kl;s} \rightarrow h_{kl;s} + \delta h_{kl;s}$ and $b_{kl} \rightarrow b_{kl} + \delta b_{kl}$ over time causes the matrix elements C_{kl} , undergo a dynamics in the matrix space. In [15], we considered a combination of multiparametric variations defined as $T \rho \equiv \sum_{k,l,s} \left[f_{kl;s} \frac{\partial \rho}{\partial h_{kl;s}} - \gamma b_{kl;s} \frac{\partial \rho}{\partial b_{kl;s}} \right]$. Using Gaussian nature of the density, it can be shown that $T \rho = L \rho$ where $L = \sum_{k,l,s} \frac{\partial}{\partial C_{kl;s}} \left[\frac{\partial \rho_c}{\partial C_{kl;s}} + \gamma C_{kl;s} \rho \right]$ and $\rho_c \propto \rho$.

As the equation $T\rho = L\rho$ is difficult to solve for generic parametric values, we seek a transformation from the set of M parameters $\{h_{kl;s}, b_{kl;s}\}$ to another set $\{y_1, \dots, y_M\}$ such that only Y_1 varies under the evolution governed by the operator T and rest of them i.e., Y_2, \dots, Y_M remain constant: $T\rho_c \equiv \frac{\partial \rho_c}{\partial y_1}$. This in turn requires

$$TY_1 = 1, \quad TY_\alpha = 0 \quad \forall \alpha > 1. \quad (\text{E1})$$

As can be seen from the definition of T given above, the contribution from the term with $b_{kl;s} \frac{\partial}{\partial b_{kl;s}} = 0$ for $b_{kl;s} = 0$ and similarly the term with $(1 - \gamma h_{kl;s}) \frac{\partial}{\partial h_{kl;s}} = 0$ as $h_{kl;s} \rightarrow \gamma^{-1}$; (we note, from eq.(7), that $\frac{\partial \rho}{\partial b_{kl;s}}$ and $\frac{\partial \rho}{\partial h_{kl;s}}$ remain well-defined in the neighbourhood of $b_{kl;s} = 0$ and $h_{kl;s} \rightarrow \gamma^{-1}$ respectively). Further $T\rho = 0$ as all $b_{kl;s} = 0$ and $h_{kl;s} \rightarrow \gamma^{-1}$; this in turn implies $\frac{\partial \rho}{\partial Y_1} = 0$ and thereby equilibrium limit of a stationary Wishart ensemble.

Using T given above, the set of equations (E1) can be solved by the standard method of characteristics, leading to

$$\frac{dh_{kk;s}}{f_{kk;s}} = \dots = \frac{db_{kl;s}}{b_{kl;s}} = dY_1 \quad (\text{E2})$$

$$\frac{dh_{kk;s}}{f_{kk;s}} = \dots = \frac{db_{kl;s}}{b_{kl;s}} = \frac{dY_n}{0} \quad n > 1 \quad (\text{E3})$$

where equality relations include all $\{kl;s\}$ pairs. The solution Y_1 of eq.(E2) is given by eq.(9) and rest of the equations give $Y_\alpha = c_k$ with c_2, \dots, c_M as the constants of evolution.

We note that a most general solution of eq.(E2) is $Y_1 = -\frac{1}{2M\gamma} \sum'_{k,l} \sum_{s=1}^{\beta} a_{kl;s} f_{kl's} + q_{kl;s} \ln |b_{kl;s}|$ with $a_{kl;s}, q_{kl;s}$ as arbitrary constants of integrations. Assuming all $f_{kl;s}$ and $b_{kl;s}$ as non-zero, we have $2N^2$ analogous differential equations to solve and resulting constants can be chosen equal i.e., $a_{kl;s} = q_{kl;s} = 1$ thereby leading to eq.(9). In case one of the $b_{kl;s} = 0$, we have $2N^2 - 1$ analogous differential equations to solve, with general solution now corresponds to $q_{kl;s} = 0$. Similarly many solution of eq.(E3) can also be found leading to different sets of basis constants.